


PML-NB-dependent type I interferon memory results in a restricted form of HSV latency

Jon B Suzich¹, Sean R Cuddy², Hiam Baidas¹, Sara Dochnal¹, Eugene Ke¹, Austin R Schinlever¹, Aleksandra Babnis¹, Chris Boutell³ & Anna R Cliffe^{1,*} 

Abstract

Herpes simplex virus (HSV) establishes latent infection in long-lived neurons. During initial infection, neurons are exposed to multiple inflammatory cytokines but the effects of immune signaling on the nature of HSV latency are unknown. We show that initial infection of primary murine neurons in the presence of type I interferon (IFN) results in a form of latency that is restricted for reactivation. We also find that the subnuclear condensates, promyelocytic leukemia nuclear bodies (PML-NBs), are absent from primary sympathetic and sensory neurons but form with type I IFN treatment and persist even when IFN signaling resolves. HSV-1 genomes colocalize with PML-NBs throughout a latent infection of neurons only when type I IFN is present during initial infection. Depletion of PML prior to or following infection does not impact the establishment latency; however, it does rescue the ability of HSV to reactivate from IFN-treated neurons. This study demonstrates that viral genomes possess a memory of the IFN response during *de novo* infection, which results in differential subnuclear positioning and ultimately restricts the ability of genomes to reactivate.

Keywords HSV; interferon; latency; neuron; PML-NB

Subject Categories Immunology; Microbiology, Virology & Host Pathogen Interaction; Neuroscience

DOI 10.15252/embr.202152547 | Received 27 January 2021 | Revised 2 June 2021 | Accepted 8 June 2021 | Published online 1 July 2021

EMBO Reports (2021) 22: e52547

See also: **SK Weller & NA Deluca** (September 2021)

Introduction

Herpes simplex virus-1 (HSV-1) is a ubiquitous pathogen that persists in the form of a lifelong latent infection in the human host. HSV-1 can undergo a productive lytic infection in a variety of cell types; however, latency is restricted to post-mitotic neurons, most commonly in sensory, sympathetic, and parasympathetic ganglia of the peripheral nervous system (Baringer & Swoveland, 1973; Warren *et al*, 1978; Baringer & Pisani, 1994; Richter *et al*, 2009).

During latent infection, the viral genome exists as an episome in the neuronal nucleus, and there is considerable evidence that on the population level viral lytic gene promoters assemble into repressive heterochromatin (Wang *et al*, 2005; Cliffe & Knipe, 2008; Cliffe *et al*, 2009; Kwiatkowski *et al*, 2009). The only region of the HSV genome that undergoes active transcription, at least in a fraction of latently infected cells, is the latency-associated transcript (LAT) locus (Stevens *et al*, 1987; Kramer & Coen, 1995). Successful establishment of a latent gene expression program requires a number of molecular events, likely influenced by both cellular and viral factors, and is not uniform (Efstathiou & Preston, 2005). Significant heterogeneity exists in expression patterns of both lytic and latent transcripts in latently infected neurons, as well as in the ability of latent genomes to reactivate in response to different stimuli (Sawtell, 1997; Proenca *et al*, 2008; Catez *et al*, 2012; Ma *et al*, 2014; Maroui *et al*, 2016; Nicoll *et al*, 2016). This heterogeneity could arise from viral genome copy number, exposure to different inflammatory environments, or intrinsic differences in the neurons themselves. Furthermore, there is growing evidence that heterogeneity in latency may ultimately be reflected in part by the association of viral genomes with different nuclear domains or cellular proteins (Catez *et al*, 2012; Maroui *et al*, 2016). However, what determines the subnuclear distribution of latent viral genomes is not known. In addition, it is currently unclear whether viral genome association with certain nuclear domains or cellular proteins results in an increased or decreased ability of the virus to undergo reactivation. The aim of this study was to determine whether the presence of interferon during initial HSV-1 infection can intersect with the latent viral genome to regulate the type of gene silencing and ultimately the ability to undergo reactivation. Because the fate of viral genomes and their ability to undergo reactivation can be readily tracked, latent HSV-1 infection of neurons also serves as an excellent system to explore how exposure to innate immune cytokines can have a lasting impact on peripheral neurons.

Latent HSV-1 genomes have been shown to associate with promyelocytic leukemia nuclear bodies (PML-NBs) in mouse models of infection, as well as in human autopsy material (Catez *et al*, 2012; Maroui *et al*, 2016). PML-NBs are heterogeneous, phase-separated nuclear condensates that have been associated with the

¹ Department of Microbiology, Immunology and Cancer Biology, University of Virginia, Charlottesville, VA, USA

² Neuroscience Graduate Program, University of Virginia, Charlottesville, VA, USA

³ MRC-University of Glasgow Centre for Virus Research (CVR), Glasgow, UK

*Corresponding author. Tel: +1 434 9247780; E-mail: cliffe@virginia.edu

transcriptional activation of cellular genes (Wang *et al*, 2004; Bernardi & Pandolfi, 2007; Lallemand-Breitenbach & de The, 2010; Kim & Ahn, 2015; McFarlane *et al*, 2019), but also can recruit repressor proteins, including ATRX, Daxx, and Sp100, that promote transcriptional repression and inhibition of both DNA and RNA virus replication (Zhong *et al*, 2000b; Garrick *et al*, 2004; Bishop *et al*, 2006; Everett & Chelbi-Alix, 2007; Xu & Roizman, 2017). In the context of lytic infection of non-neuronal cells, PML-NBs have been shown to closely associate with HSV-1 genomes (Maul *et al*, 1996; Maul, 1998), and the HSV-1 viral regulatory protein ICP0 is known to disrupt the integrity of these structures by targeting PML and other PML-NB-associated proteins for degradation (Everett & Maul, 1994; Chelbi-Alix & de The, 1999; Boutell *et al*, 2002). PML-NBs entrapment of HSV-1 genomes during lytic infection of fibroblasts (Alandijany *et al*, 2018) is hypothesized to create a transcriptionally repressive environment for viral gene expression, as PML directly contributes to the cellular repression of ICP0-null mutant viruses (Everett *et al*, 2006). In the context of latency, neurons containing PML-encased latent genomes exhibit decreased expression levels of the LAT (Catez *et al*, 2012), suggesting that they are more transcriptionally silent than latent genomes localized to other nuclear domains and raising the question as to whether PML-NB-associated genomes are capable of undergoing reactivation. Studies have shown that replication-defective HSV genomes associated with PML-NBs are capable of derepressing following induced expression of ICP0 in fibroblasts (Everett *et al*, 2007; Cohen *et al*, 2018) and following addition of the histone deacetylase inhibitor trichostatin A (TSA) in cultured adult TG neurons (Maroui *et al*, 2016). However, it is not known if replication-competent viral genomes associated with PML-NBs are capable of undergoing reactivation triggered by activation of cellular signaling pathways in the absence of viral protein.

PML-NBs can undergo significant changes in number, size, and localization depending on cell type, differentiation stage, and cell-cycle phase, as well as in response to cellular stress and soluble factors (Bernardi & Pandolfi, 2007; Lallemand-Breitenbach & de The, 2010). Interferon (IFN) treatment directly induces the transcription of PML, Daxx, Sp100, and other PML-NB constituents, which leads to elevated protein synthesis and a robust increase in both size and number of PML-NBs (Chelbi-Alix *et al*, 1995; Stadler *et al*, 1995; Grotzinger *et al*, 1996; Greger *et al*, 2005; Shalginskikh *et al*, 2013). During HSV-1 infection, type I IFNs are among the first immune effectors produced, and they have been shown to restrict HSV viral replication and spread both *in vitro* and *in vivo* through multiple pathways (Hendricks *et al*, 1991; Mikloska *et al*, 1998; Mikloska & Cunningham, 2001; Sainz & Halford, 2002; Jones *et al*, 2003). Type I IFNs are elevated within peripheral ganglia during HSV-1 infection (Carr *et al*, 1998) and have been linked with control of lytic HSV-1 replication. In an *in vitro* model of latency, exogenous type I IFNs also have been shown to induce neuron-specific antiviral responses that control reactivation (Linderman *et al*, 2017), but whether type I IFN exposure during initial infection modulates entry into latency is not known. Importantly, exposure to IFN and other cytokines has also been shown to generate innate immune memory or “trained immunity” in fibroblasts and immune cells (Kamada *et al*, 2018; Moorlag *et al*, 2018), and PML-NBs themselves are potentially important in the host innate immune response. A previous study found that the histone chaperone HIRA is re-localized to PML-NBs

in response to the innate immune defenses induced by HSV-1 infection, and in this context, PML was required for the recruitment of HIRA to ISG promoters for efficient transcription (McFarlane *et al*, 2019). Prior exposure to type I interferons has also been shown to promote a transcriptional memory response in fibroblasts and macrophages (Kamada *et al*, 2018). This interferon memory leads to faster and more robust transcription of ISGs following restimulation and coincided with acquisition of certain chromatin marks and accelerated recruitment of transcription and chromatin factors (Kamada *et al*, 2018). Thus far, long-term memory of cytokine exposure has only been investigated in non-neuronal cells, but it is conceivable that neurons, being non-mitotic and long-lived cells, also possess unique long-term responses to prior cytokine exposure.

Although *in vivo* models are incredibly powerful tools to investigate the contribution of the host immune response to HSV infection, they are problematic for investigating how individual components of the host’s immune response specifically regulate neuronal latency. Conversely, *in vitro* systems provide a simplified model that lacks many aspects of the host immune response. Therefore, to investigate the role of type I IFN on HSV-1 latency and reactivation, we utilized a model of latency in primary murine sympathetic neurons (Cliffe *et al*, 2015), which allowed us to manipulate conditions during initial HSV-1 infection and trigger synchronous robust reactivation. Using this model, we show that primary neurons isolated from mouse peripheral ganglia are largely devoid of detectable PML-NBs but PML-NBs form following type I IFN exposure and persist even when ISG gene expression and production of other antiviral proteins have returned to baseline. Neither exogenous type I IFN nor detectable PML-NBs are required for HSV gene silencing and entry into latency in this model system, but, importantly, the presence of IFN α specifically at the time of initial infection results in the entrapment of viral genomes in PML-NBs and a more restrictive form of latency that is less able to undergo reactivation. This study therefore demonstrates how the viral latent genome has a long-term memory of the innate response during *de novo* HSV infection that results in entrapment of genomes in PML-NBs and a more repressive form of latency.

Results

Interferon induces the formation of detectable PML-NBs in primary sympathetic and sensory neurons isolated from postnatal and adult mice

We initially set out to investigate the contribution of PML-NBs to HSV latency and reactivation using primary sympathetic and sensory neurons that have been well characterized as *in vitro* models of HSV latency and reactivation (Wilcox & Johnson, 1987; Wilcox *et al*, 1990; Camarena *et al*, 2010; Cliffe *et al*, 2015; Ives & Bertke, 2017; Cuddy *et al*, 2020). In addition, primary neuronal systems allow for much more experimental control of specific conditions during *de novo* infection and can be easily manipulated either immediately prior to or following infection. Peripheral neurons were isolated from the superior cervical ganglia (SCG) or trigeminal ganglia (TG) from young (post-natal day; P1) or adult (> P28) mice and cultured for 6 days prior to staining. PML-NBs were defined as detectable punctate nuclear structures by staining for PML protein.

Strikingly, we observed that both SCG and TG neurons were largely devoid of detectable PML-NBs (Fig 1A).

In certain cell types, the transcription of certain PML-NB-associated proteins, including PML, can be induced by either type I or type II interferon (IFN) treatment, which is correlated with an increase in PML-NB size and/or number per cell (Chelbi-Alix *et al*, 1995; Stadler *et al*, 1995). Therefore, we were interested in determining whether exposure of primary sensory or sympathetic neurons to different types of IFN resulted in PML-NB formation. Type I IFN treatment using IFN- α (IFN α) (Fig 1B, C–F) or IFN- β (Fig EV1A) led to a significant induction of detectable PML-NBs in both sensory and sympathetic neurons isolated from postnatal and adult mice. Representative images of IFN α -treated neurons are shown (Fig 1B), and the number of detectable PML-NBs per neuron is quantified (Fig 1C–F). The increase in detectable PML-NBs was comparable for both 150 IU/ml and 600 IU/ml of IFN α . Type II IFN (IFN γ) led to a more variable response with a small but significant increase in detectable PML-NBs in a subpopulation of sympathetic neurons. However, IFN γ treatment of sensory neurons did not result in the formation of detectable PML-NBs. Exposure of neurons to IFN- λ 2 (IFN- λ 2), a type III IFN, did not induce the formation of detectable PML-NBs in either sympathetic or sensory neuron cultures (Figs 1C–F and EV1B and C). Therefore, PML-NBs are largely undetectable in primary sympathetic and sensory neurons but can form upon exposure to type I IFNs.

The absence of detectable PML-NBs in untreated primary neurons prompted us to investigate other known components of PML-NBs. We were particularly interested in ATRX and Daxx because like PML they have previously been found to be involved in restricting HSV lytic replication in non-neuronal cells (Lukashchuk & Everett, 2010; Alandijany *et al*, 2018; Cabral *et al*, 2018; McFarlane *et al*, 2019). Therefore, we investigated the localization of ATRX and Daxx in primary peripheral neurons. ATRX is a multifunctional, heterochromatin-associated protein that is localized to PML-NBs in human and mouse mitotic cells and is largely characterized as interacting with the Daxx histone chaperone (Lewis *et al*, 2010; Clynes *et al*, 2013). In untreated neurons, we observed abundant ATRX staining throughout the nucleus in regions that also stained strongly with Hoechst (Fig EV1D and E). This potential colocalization of ATRX with regions of dense chromatin is consistent with a previous study demonstrating that in neurons ATRX binds certain regions of the cellular genome associated with the constitutive heterochromatin modification H3K9me3 (Noh *et al*, 2015). Importantly, this distribution of ATRX differs from what is seen in murine dermal fibroblasts (Fig EV1D and E) and other non-neuronal cells, where there is a high degree of colocalization between ATRX and PML (Alandijany *et al*, 2018). Following treatment with IFN α , we found a redistribution of ATRX staining and colocalization between ATRX and the formed PML-NBs, but the majority of ATRX staining remained outside the context of PML-NBs (Fig EV1D and E). Similar to PML, sympathetic SCG and sensory TG neurons isolated from both postnatal and adult mice were devoid of detectable puncta of Daxx staining (Fig EV1E), and we did not observe extensive Daxx staining in untreated neurons as we did for ATRX. We were unable to directly co-stain for Daxx and PML; however, treatment of neurons with IFN α did induce punctate Daxx staining that strongly colocalized with puncta of ATRX (Fig EV1E), which given our previous observation of ATRX colocalization with

PML following type I IFN treatment we used as a correlate for PML-NBs. We were also interested in SUMO-1, which has been shown to be required for formation of PML-NBs (Zhong *et al*, 2000a). Similar to ATRX and Daxx, treatment of neurons with IFN α induced punctate SUMO-1 staining in P6 SCG neurons that colocalized with PML puncta (Fig EV1F). Therefore, PML-NBs containing their well-characterized associated proteins are not detected in cultured primary neurons but form in response to type I IFN exposure.

Type I IFN treatment specifically at time of infection restricts reactivation of HSV-1 from primary sympathetic neurons without affecting initial infectivity or LAT expression

Because we observed that primary SCG neurons are largely devoid of PML-NBs and that PML-NBs form upon treatment with type I IFN treatment, we first wanted to clarify that latency was maintained in the absence of IFN and presumably without PML-NB formation, consistent with our previous data (Cuddy *et al*, 2020). SCG neurons were infected at a multiplicity of infection (MOI) of 7.5 plaque forming units (PFU)/cell with HSV-1 Us11-GFP presence of acyclovir (ACV). The ACV was removed after 6 days, and the neuronal cultures were monitored to ensure the no GFP-positive neurons were present (Fig 2A). We found that latency could be established and maintained for up to 5 days following removal of ACV (Fig 2B). Reactivation was triggered by PI3K inhibition using LY294002, as previously described (Camarena *et al*, 2010; Kim *et al*, 2012; Kobayashi *et al*, 2012; Cliffe *et al*, 2015), and quantified based on the number of Us11-GFP neurons in the presence of WAY-150138 which blocks packaging of progeny genomes and thus cell-to-cell spread (van Zeijl *et al*, 2000). These data therefore indicate that exogenous IFN is not required to induce a latent state in this model system.

We next turned our attention to whether type I IFN treatment at the time of infection impacted the ability of HSV to establish latency or reactivate in this model system. SCG neurons were pretreated with IFN α (600 IU/ml) for 18 h and during the initial 2 h HSV inoculation. Following inoculation, IFN α was washed out and an IFNAR1 blocking antibody was used to prevent subsequent type I IFN signaling through the receptor. To confirm the effectiveness of the IFNAR1 ab to block detectable IFN signaling, we validated it by its ability to block ISG expression (ISG15) in cultured SCG neurons by RT-qPCR (Fig EV2A). Reactivation was induced and initially quantified based on the number of GFP-positive neurons at 3 days post-stimuli. We found that full reactivation was restricted in neurons exposed to type I IFN just prior to and during *de novo* infection (Fig 2C). We further confirmed this IFN α -mediated restriction of latency by the induction of lytic mRNAs upon reactivation. IFN α treatment at the time of infection significantly decreased the expression of immediate-early gene (ICP27), early gene (ICP8), and late gene (gC) at 3 days post-reactivation (Figs 2D and EV2AB and C). There were very few GFP-positive neurons and little to no viral gene expression in mock reactivated controls, further indicating that latency can be established in the presence and absence of IFN.

Reactivation of HSV in this system proceeds over two phases. GFP-positive neurons is a readout for full reactivation or Phase II. However, we and others have observed an initial wave of lytic gene expression that occurs prior to and independently of viral DNA replication at around 20 h post-stimulus, termed Phase I (Du *et al*, 2011; Kim *et al*, 2012; Cliffe *et al*, 2015; Cliffe & Wilson, 2017). Therefore,

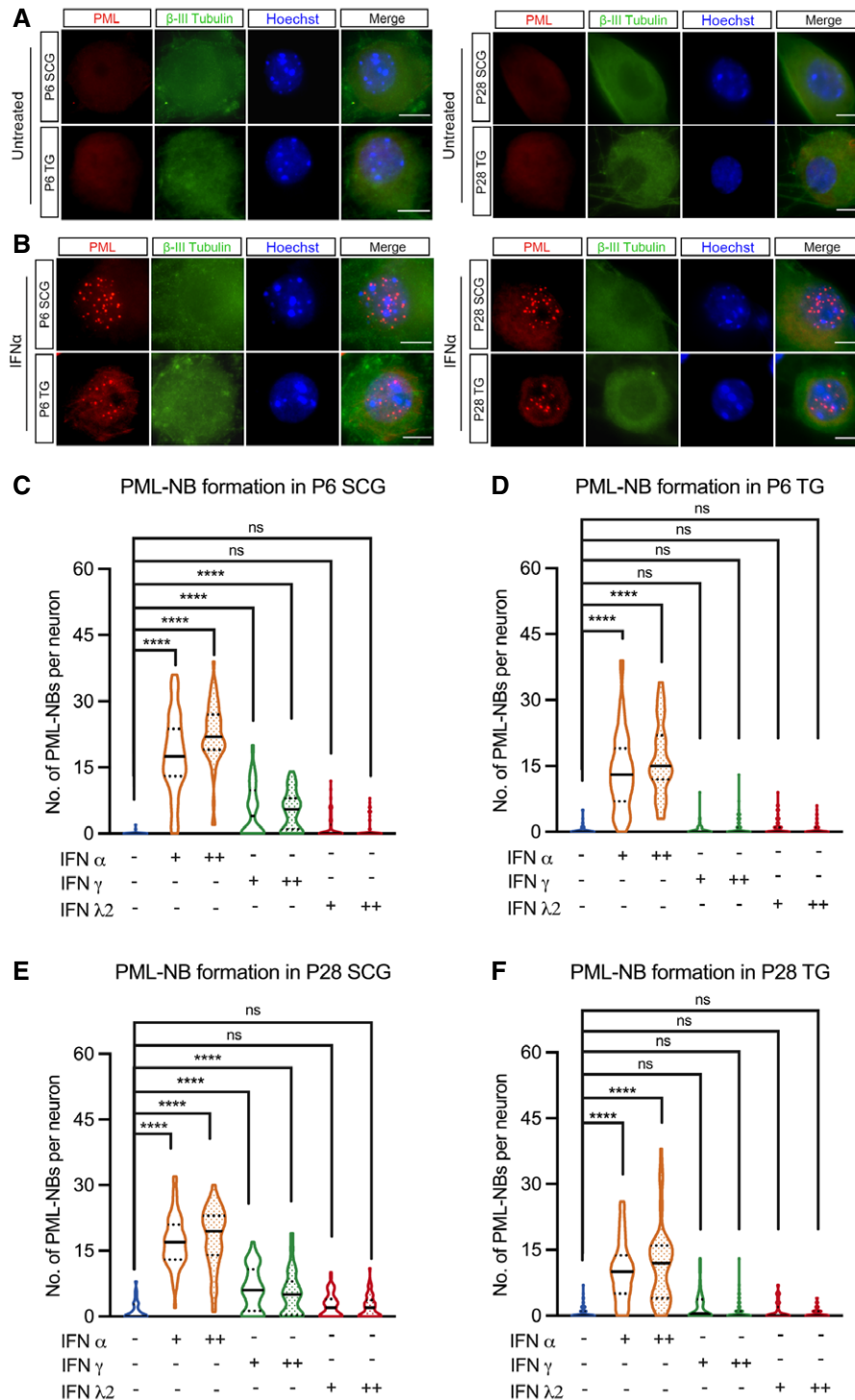


Figure 1. Type I IFN induces the formation of PML-NBs in primary peripheral neurons.

A Representative images of primary neurons isolated from superior cervical ganglia (SCG) and sensory trigeminal ganglia (TG) of postnatal (P6) and adult (P28) mice stained for PML and the neuronal marker BIII-tubulin.

B SCG and TG neurons isolated from P6 and P28 mice were treated with interferon (IFN) α (600 IU/ml) for 18 h and stained for PML and BIII-tubulin.

C–F Quantification of detectable PML puncta in P6 and P28 neurons following 18-h treatment with IFN α (150 IU/ml, 600 IU/ml), IFN γ (150 IU/ml, 500 IU/ml), and IFN λ 2 (100 ng/ml, 500 ng/ml). Data information: Data represent the mean \pm SEM. $n = 60$ cells from 3 biological replicates. Statistical comparisons were made using a one-way ANOVA with Tukey's multiple comparison (ns not significant, **** $p < 0.0001$). Scale bar, 20 μ m.

Source data are available online for this figure.

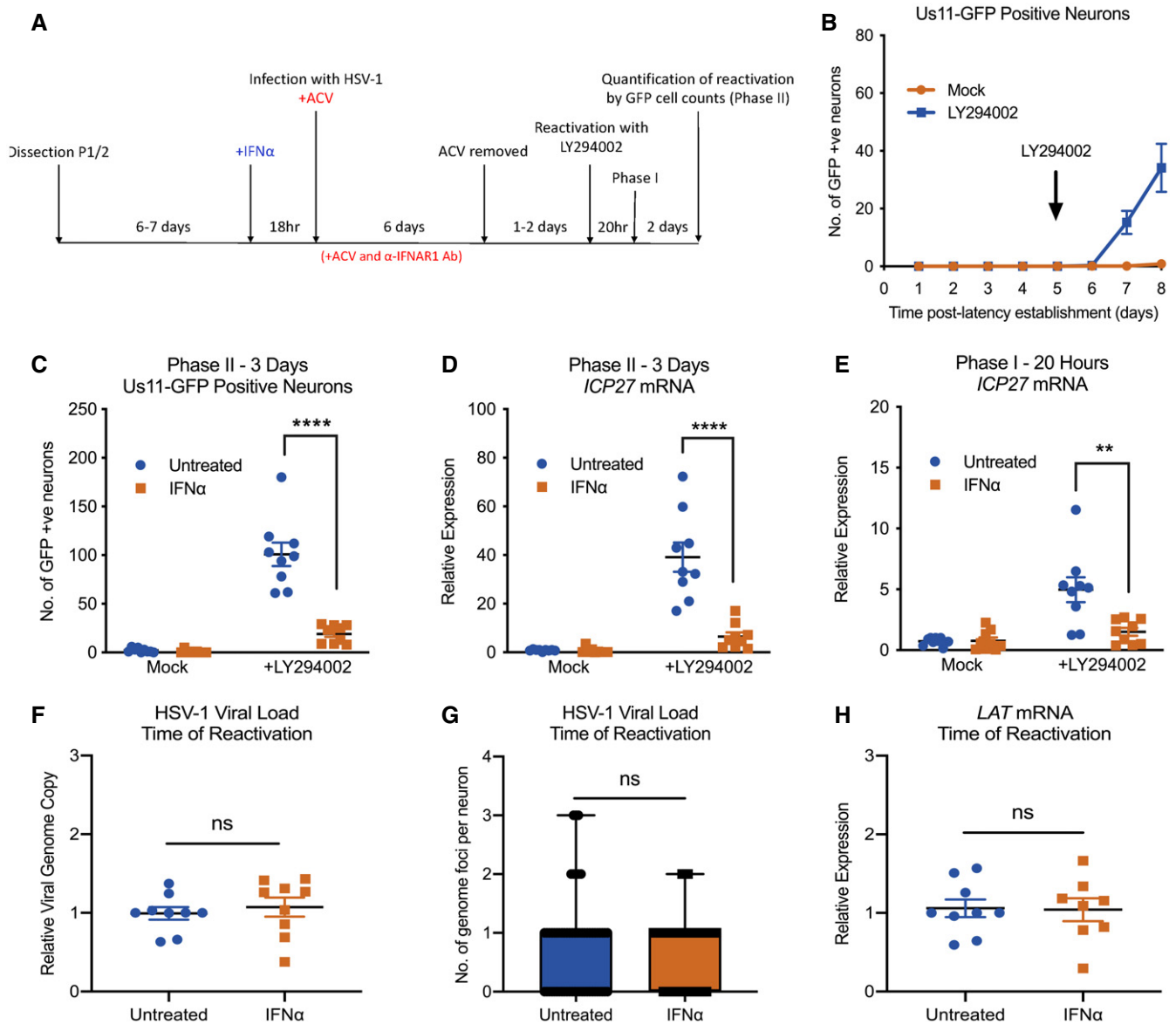


Figure 2. Type I IFN treatment solely at time of infection inhibits LY294002-mediated reactivation of HSV-1 in primary sympathetic SCG neurons.

A Schematic of the primary postnatal sympathetic neuron-derived model of HSV-1 latency.

B Reactivation from latency is quantified by Us11-GFP expressing neurons following addition of the PI3K inhibitor LY294002 (20 μ M) in the presence of WAY-150168, which prevents cell-to-cell spread. The arrow indicates the time of LY294002 treatment at 5 days post-establishment of latency. $n = 9$ biological replicates.

C Number of Us11-GFP expressing neurons at 3 days post-LY294002-induced reactivation in P6 SCG neuronal cultures infected with HSV-1 in the presence or absence of IFN α (600 IU/ml), then treated with an α -IFNAR1 neutralizing antibody. $n = 9$ biological replicates.

D RT-qPCR for viral mRNA transcripts at 3 days post-LY294002-induced reactivation of SCGs infected with HSV-1 in the presence or absence of IFN α . $n = 9$ biological replicates.

E RT-qPCR for viral mRNA transcripts at 20 h post-LY294002-induced reactivation in SCGs infected with HSV-1 in the presence or absence of IFN α . $n = 9$ biological replicates.

F Relative amount of viral DNA at time of reactivation (8 dpi) in SCG neurons infected with HSV-1 in the presence or absence of IFN α (600 IU/ml). $n = 9$ biological replicates.

G Quantification of vDNA foci detected by click chemistry at time of reactivation (8 dpi) in SCG neurons infected with HSV-1 in the presence or absence of IFN α (600 IU/ml). $n = 60$ genomes from 3 biological replicates.

H LAT mRNA expression at time of reactivation (8 dpi) in neurons infected with HSV-1 in the presence or absence of IFN α (600 IU/ml). $n = 9$ biological replicates.

Data information: Data represent the mean \pm SEM. Statistical comparisons were made using a Mann-Whitney test (ns not significant, ** $P < 0.01$, **** $P < 0.0001$).

Source data are available online for this figure.

to determine whether IFN α treatment at the time of infection restricted the Phase I wave of lytic, we carried out RT-qPCR to detect representative immediate-early (ICP27), early (ICP8), and late (gC) transcripts at 20 h post-addition of LY294002. We found significantly decreased expression in the IFN α -treated neurons (Figs 2E and EV2D and E). This is interesting as exogenous type I IFNs have previously been shown to suppress reactivation in murine neurons by preventing Phase I and are rendered ineffective once Phase I viral products accumulate (Linderman *et al*, 2017). Therefore, type I IFN treatment solely at the time of infection has a long-term effect on the ability of HSV to initiate lytic gene expression and undergo reactivation.

Because IFN treatment could reduce nuclear trafficking of viral capsids during initial infection or impact infection efficiency, we next determined whether equivalent numbers of viral genomes were present in the neuronal cultures. At 8 dpi, we measured relative viral DNA genome copy numbers in SCG neurons that were treated with IFN α compared to untreated controls and found no significant difference (Fig 2F). To further confirm that equivalent genomes were present in the neuronal nuclei, we infected neurons with HSV-1-containing EdC-incorporated genomes and performed click chemistry to detect vDNA foci. At 8 dpi, we found no significant difference in the average number of vDNA foci per nucleus of neurons treated with IFN α at the time of initial infection compared to untreated controls (Fig 2G). Therefore, the restricted reactivation phenotype mediated by IFN α was not due to a decrease in the number of latent viral genomes.

The decreased reactivation observed with IFN α treatment could be secondary to changes in expression of the LAT and/or directly as a result of decreased viral genome accessibility. The HSV LAT, one of the only highly expressed gene products during latent infection, has been shown to modulate several features of latency, including the viral chromatin structure, lytic gene expression, and neuronal survival, as well as the efficiency of latency establishment and reactivation (Leib *et al*, 1989; Hill *et al*, 1990; Trousdale *et al*, 1991; Gordon *et al*, 1995; Chen *et al*, 1997; Garber *et al*, 1997; Thompson & Sawtell, 1997, 2001; Perng *et al*, 2000; Knipe & Cliffe, 2008). Therefore, the ability of HSV to undergo reactivation could be due to changes in LAT expression following IFN α treatment. However, when we evaluated LAT expression levels at 8 dpi by RT-qPCR, we found no detectable difference between IFN α -treated and untreated cultures of neurons. This suggests that the IFN α -mediated restriction in reactivation does not appear to occur as a result of changes in expression of the LAT (Fig 2H). Therefore, it is possible that the type I IFN-mediated restriction of HSV latency is due to changes to the latent genome that results in a decreased ability to undergo reactivation following PI3-kinase inhibition.

Primary neurons have a memory of prior IFN α exposure characterized by persistence of PML-NBs

Because we observed a restriction in the ability of HSV to reactivate that occurred 7–8 days following type I IFN exposure, we went on to examine any long-term changes resulting from IFN α exposure. First, we investigated the kinetics of representative ISG expression. As expected, we saw a robust induction of *Isg15* and *Irf7* in IFN α -treated (600 IU/ml) neurons that persisted for at least 42 h post-treatment post-addition of IFN α (this represents 1 day post-infection (dpi)). However, by 8 dpi, the time at which neurons were induced

to reactivate, there was no detectable difference in *Isg15* or *Irf7* expression in IFN α -treated neurons vs untreated controls (Fig 3A and B), indicating that these representative ISGs were not detectably elevated at the time of reactivation. We also found similar *Isg15* and *Irf7* expression in HSV-1-infected neurons compared to uninfected controls, suggesting that HSV-1 infection was not impacting IFN signaling pathways at a population level. PML has been previously characterized as an ISG product in non-neuronal cells (Chelbi-Alix *et al*, 1995; Stadler *et al*, 1995) and is responsive to both IFN β and IFN γ in latently infected rat sympathetic neurons induced to reactivate (Linderman *et al*, 2017), and we found an approximate 5-fold increased expression of *Pml* in primary sympathetic neurons following IFN α treatment which was less than the increased expression of *Irf7* and *Isg15* (approximate 250-fold and 100-fold increased expression, respectively). *Pml* expression returned to untreated levels by 1 dpi (Fig 3C).

Although we did not detect maintained induction of IFN-stimulated gene expression including *Pml*, we were intrigued as to whether PML-NBs persisted throughout the course of infection. To assess this, we first established whether PML-NBs persist even in the absence of sustained ISG expression. Quantifying the number of PML-NBs following IFN α (600 IU/ml) treatment, we found that the number of bodies remains elevated through 15 days post-treatment (Fig 3D). We went on to investigate additional products of ISGs including STAT1 and Mx1 because of the availability of specific antibodies against these proteins. We observed robust STAT1 staining following IFN α exposure for 18 h. However, by 8 days post-infection, we could not detect STAT1 staining in primary neurons indicating that accumulation of this IFN α -induced protein had returned to baseline (Fig 3E). Similarly, we found induction of punctate Mx1 staining in neurons exposed to IFN α for 18 h that was undetectable by day 6 post-treatment (Fig 3F). Therefore, exposure of primary neurons to type I IFN led to a modest induction of *Pml* mRNA but resulted in long-term persistence of PML-NBs, even in the absence of continued IFN signaling and when antiviral protein products of other ISGs were undetectable.

PML-NBs persist and stably entrap latent HSV-1 genomes only if IFN α is present at the time of initial infection

The persistence of PML-NBs following IFN exposure raised the possibility that viral genomes are maintained within PML-NBs only in type I IFN-treated neurons. This would also suggest that PML-NB-associated genomes are less permissive for reactivation and provide us with an experimental system to investigate the contribution of PML-NBs to the maintenance of HSV latency. To determine whether viral genomes localize with PML-NBs in type I IFN-treated neurons, SCG neurons were pretreated with IFN α (600 IU/ml) then infected with HSV-1^{EdC} at an MOI of 5 PFU/cell in the presence of ACV and IFN α as described above. By co-staining for PML, we found that a large proportion of vDNA foci colocalized with PML-NBs in the IFN α -treated neurons over the course of infection. In untreated neurons that are largely devoid of detectable PML-NBs, very few genomes were colocalized to PML puncta as expected. Representative images are shown (Fig 4A) and the percent of genome foci colocalized to PML-NBs is quantified (Fig 4B). Furthermore, high-resolution Airy scan-based 3D confocal microscopy of IFN α -treated neurons revealed that vDNA foci were entrapped within PML-NBs

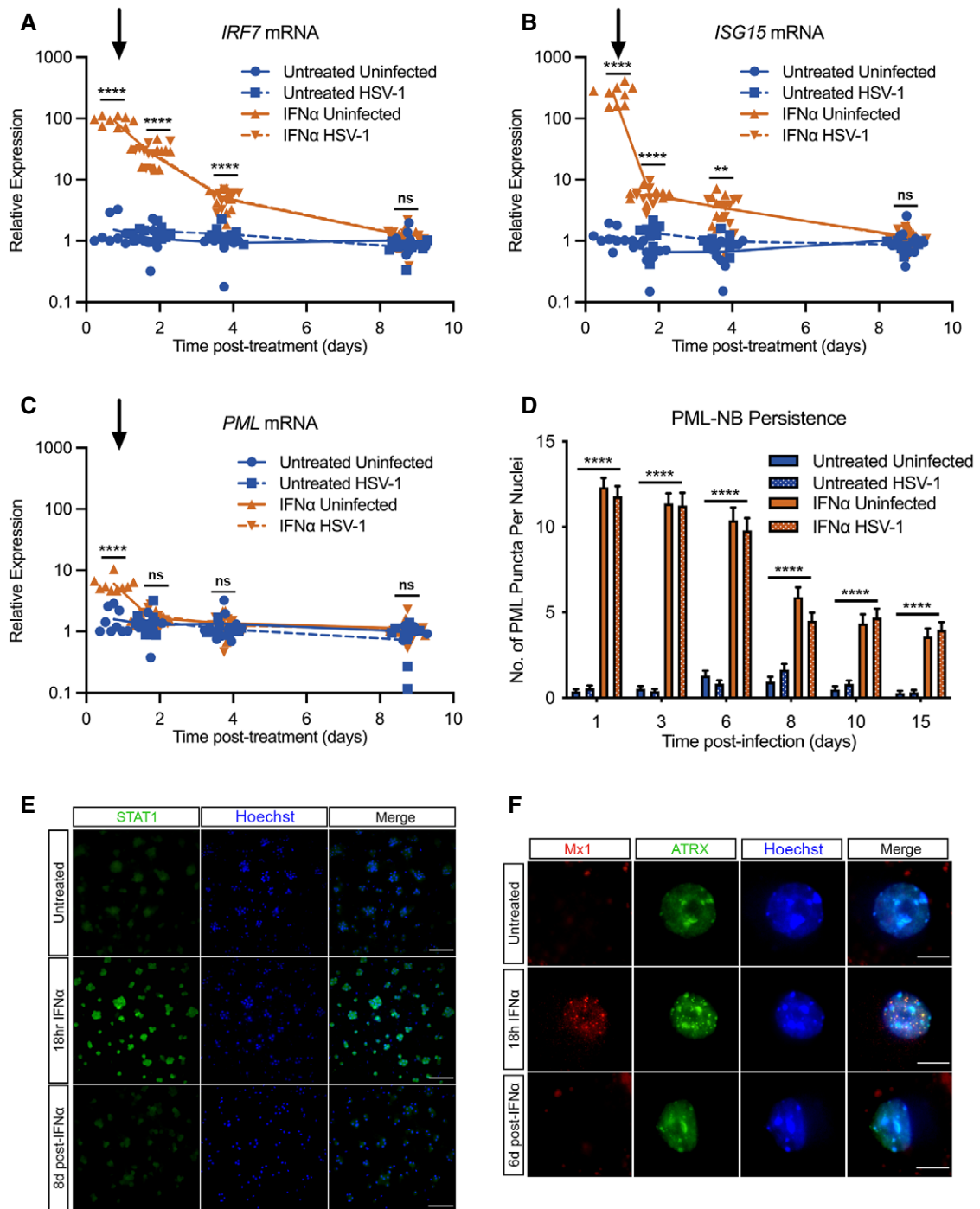


Figure 3. Type I IFN-induced PML-NBs persist in primary sympathetic neurons despite resolution of IFN signaling.

A–C Kinetics of *ISG15*, *IRF7*, and *PML* mRNA expression at 0.75, 1.75, 3.75, and 8.75 days post-IFN α (600 IU/ml) treatment. Arrow indicates the time of HSV-1 infection at 18 h post-interferon treatment. $n = 9$ biological replicates.

D Quantification of PML puncta at 1, 3, 6, 8, 10 and 15 days post-infection with HSV-1 in untreated and IFN α (600 IU/ml)-treated SCG neurons. $n \geq 60$ cells from 3 biological replicates.

E Representative images of P6 SCG neurons treated with IFN α (600 IU/ml) and stained for STAT1 at 18 h and 8 days post-treatment. Scale bar, 100 μ m.

F Representative images of P6 SCG neurons treated with IFN α (600 IU/ml) and stained for Mx1 at 18 h and 6 days post-treatment. Scale bar, 20 μ m.

Data information: Data represent the mean \pm SEM. Statistical comparisons were made using one-way ANOVA with Tukey's multiple comparison (A–C) or mixed-effects analysis with Tukey's multiple comparison (D). (ns not significant, ** $P < 0.01$, **** $P < 0.0001$).

Source data are available online for this figure.

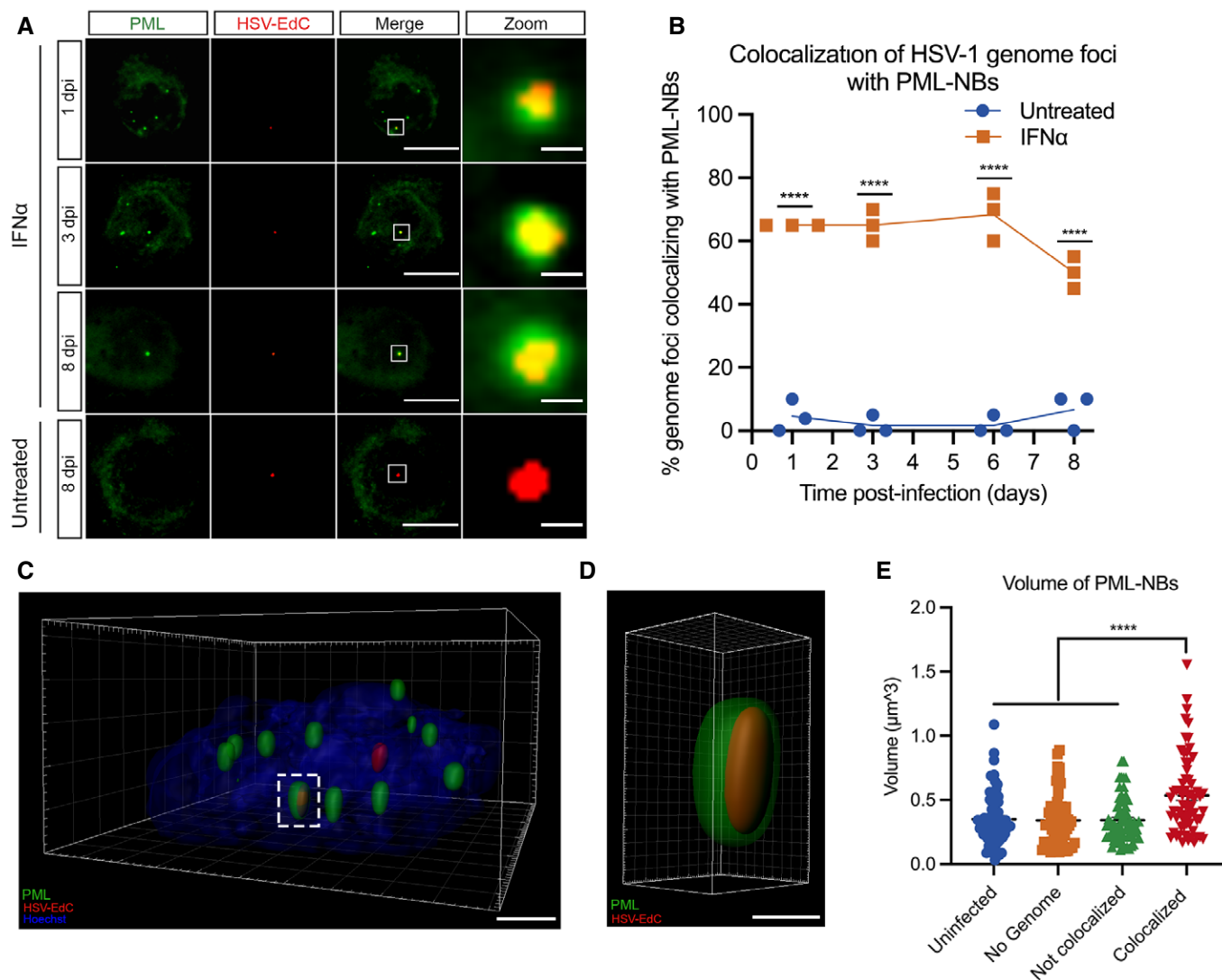


Figure 4. Type I IFN-induced PML-NBs stably entrap vDNA throughout a latent HSV-1 infection of primary sympathetic neurons.

- A** Representative images of vDNA foci detected by click chemistry to PML at 1, 3, 6, and 8 dpi in P6 SCG neurons infected with HSV-1^{EdC} in the presence or absence of IFN α (600 IU/ml). Z-stack images of individual vDNA foci were acquired. Scale bar, 20 μ m. Zoom scale bar, 1 μ m.
- B** Percent colocalization of vDNA foci detected by click chemistry to PML at 1, 3, 6, and 8 dpi in SCG neurons infected with HSV-1^{EdC} in the presence or absence of IFN α (600 IU/ml). Each point represents the percentage of 20 vDNA foci that colocalized to PML from 3 biological replicates.
- C, D** (C) 3D reconstruction of a high-resolution Z-series confocal image showing PML entrapment of a HSV-1^{EdC} vDNA foci. Scale bar, 2 μ m. (D) Enlargement of PML entrapped vDNA outlined by white dashed box. Scale bar, 0.5 μ m.
- E** Quantification of PML-NB volume in SCG neurons infected with HSV-1^{EdC} in the presence or absence of IFN α (600 IU/ml). $n = 64$ biological replicates.

Data information: Data represent the mean \pm SEM. Statistical comparisons were made using a 2-way ANOVA (B) or a one-way ANOVA with Tukey's multiple comparison (E) (**** $P < 0.0001$).

Source data are available online for this figure.

(Fig 4C and D), as has also been reported upon lytic infection of non-neuronal cell lines (Alandijany *et al*, 2018) and in latently infected TG *in vivo* (Catez *et al*, 2012), and interestingly, we found that the volume of PML-NBs associated with vDNA is greater than PML-NBs not associated with vDNA (Fig 4E). Previous studies have found that colocalization of viral DNA by PML-NBs during lytic HSV-1 infection of human fibroblasts occurs independently of type I IFN exposure (Maul *et al*, 1996; Everett *et al*, 2004; Everett & Murray, 2005; Alandijany *et al*, 2018), and we confirmed this was

also the case in dermal fibroblasts isolated from postnatal mice (Fig EV3A and B). Therefore, the presence of IFN α during initial infection can impact the long-term subnuclear localization of latent viral genomes in neurons by inducing PML-NBs that persist and stably entrap latent viral genomes.

Thus far, our data indicate that the presence of IFN α during initial infection determines subnuclear positioning of latent viral genomes and the ability of genomes to reactivate in response to inhibition of PI3-kinase activity. We considered that type I IFN

treatment could have a long-term effect on cell signaling pathways which could impact the ability of HSV to reactivate. Therefore, to determine the direct versus indirect effects on the viral genome itself, we next investigated whether the timing of IFN α exposure had a differential effect on the ability of viral genomes to reactivate. We treated postnatal SCG neurons with IFN α (600 IU/ml) for 18 h and during the 2 h HSV inoculation (–18 hpi) or exposed neurons to IFN α for 18 h at 3 days prior to infection (–3 dpi). Following pretreatment at –3 dpi or –18 hpi, IFN α was washed out and an IFNAR1 blocking antibody was used. As expected, IFN α during initial infection significantly inhibited HSV reactivation, but surprisingly, IFN α treatment at –3 dpi did not restrict reactivation as shown by the similar number of GFP-positive neurons at 72 h post-reactivation when compared to untreated neurons (Fig 5A).

Consistent with the reactivation data, we found that vDNA foci did not localize to PML-NBs in SCG neurons treated with IFN α at –3 dpi (Fig 5B). We confirmed that PML-NBs were present at the time of infection in neurons treated 3 days prior to infection (Fig 5C), although we did detect slightly fewer PML-NBs per nucleus in neurons treated –3 dpi compared to –18 hpi (a mean of 17.57 versus 12.47 per nucleus, respectively). We also confirmed comparable recruitment of known PML-NB-associated proteins ATRX, Daxx, and SUMO-1 at 3 days post-IFN α treatment (Fig EV4A–C). When IFN α treatment of SCG neurons is continued from –3 dpi through infection, or if SCG neurons treated at –3 dpi receive a second treatment of IFN α during infection, then a similar proportion of latent viral genomes colocalize with PML-NBs as with a single treatment during infection (Fig EV4D). Together with the previous

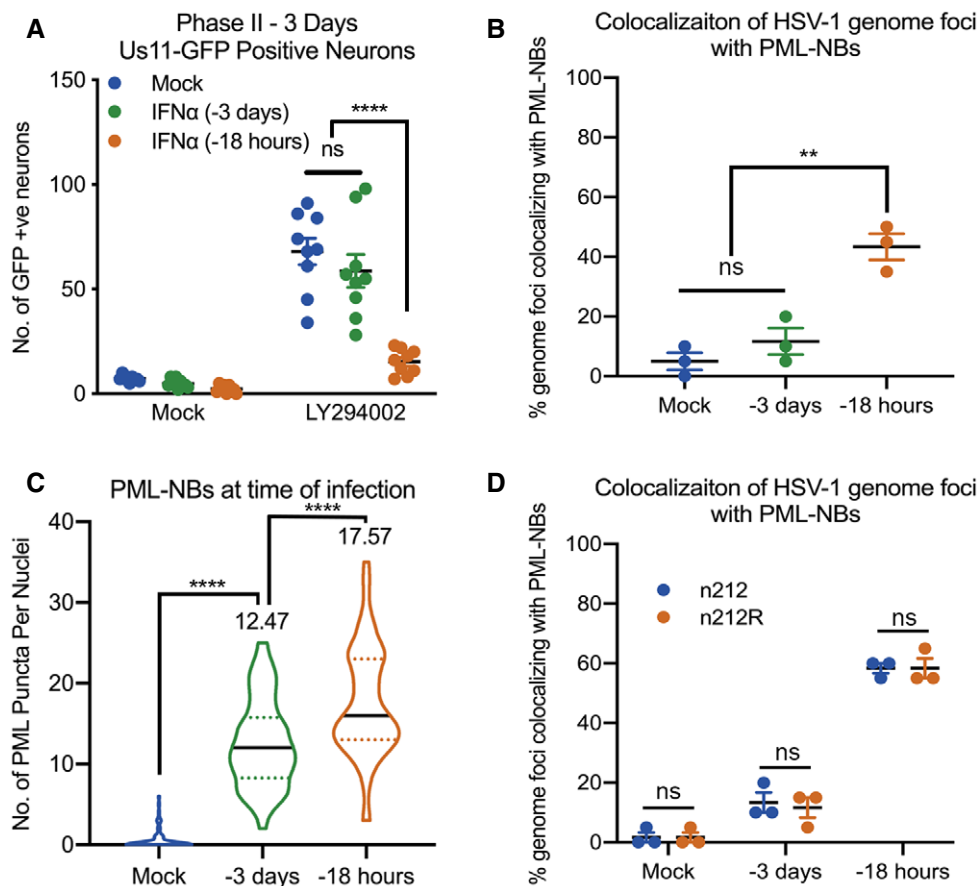


Figure 5. HSV-1 genomes only associate with PML-NBs when type I IFN is present during initial infection.

- A Number of Us11-GFP expressing P6 SCG neurons infected with HSV-1 following IFN α treatment for 18 h prior to infection or for 18 h at 3 days prior to infection. $n = 9$ biological replicates.
- B Percent colocalization of vDNA foci detected by click chemistry to PML at 8 dpi in SCG neurons infected with HSV-1^{EdC} following IFN α treatment for 18 h prior to infection or for 18 h at 3 days prior to infection. Each point represents the percentage of 20 vDNA foci that colocalized to PML from 3 biological replicates.
- C Quantification of PML puncta at time of infection in P6 SCG neurons treated with IFN α (600 IU/ml) for 18 h prior to infection or for 18 h at 3 days prior to infection. $n = 60$ cells from 3 biological replicates.
- D Percent colocalization of vDNA foci detected by click chemistry to PML at 3 dpi in SCG neurons with HSV-1^{EdC} infected with ICPO-null mutant HSV-1, n212, or a rescued HSV-1 virus, n212R, in P6 SCG neurons treated with IFN α for 18 h prior to infection or for 18 h at 3 days prior to infection. Each point represents the percentage of 20 vDNA foci that colocalized to PML from 3 biological replicates.

Data information: Data represent the mean \pm SEM. Statistical comparisons were made using a one-way ANOVA with Tukey's multiple comparison (A–C) or a 2-way ANOVA (D) (ns not significant, ** $P < 0.01$, **** $P < 0.0001$).

Source data are available online for this figure.

data on genome entrapment in dermal fibroblasts (Fig EV3A and B), these data indicate that type I IFN must be present during infection of neurons, but not necessarily non-neuronal cells, for ν DNA to colocalize with PML-NBs.

The HSV-infected cell protein 0 (ICP0) is a RING-finger E3 ubiquitin ligase that is synthesized at very early stages of HSV-1 infection (Boutell *et al*, 2002). During lytic infection, it localizes to PML-NBs and disrupts their integrity by targeting PML and other PML-NB-associated proteins for degradation (Everett *et al*, 1998; Muller *et al*, 1998; Chelbi-Alix & de The, 1999; Boutell *et al*, 2002; Boutell *et al*, 2011; Cuchet-Lourenco *et al*, 2012; Alandijany *et al*, 2018). This activity is required for promoting the efficient onset of HSV-1 lytic replication, and ICP0-null mutants exhibit a defect in viral gene expression in certain cell types at low multiplicities of infection (Everett *et al*, 2008). ICP0 mRNA is also known to be expressed during the establishment of latency (Cliffe *et al*, 2013). Therefore, the colocalization of latent viral genomes to PML-NBs and ultimately the ability of HSV to undergo reactivation could be due the presence of IFN α during initial infection and its effect on the localization or amount of ICP0. To investigate the distribution of ICP0 at early time points post-infection, SCG neurons were treated with IFN α at either -3 dpi or -18 hpi and infected at a MOI of 7.5 PFU/cell with HSV-1 Us11-GFP in the presence of acyclovir (ACV). In both treatment groups, ICP0 staining similarly colocalized with puncta of ATRX, a correlate for PML-NBs, at 3, 6, and 9 h post-infection (Fig EV4E and F). Interestingly, foci of ATRX still remained even with the presence of ICP0, suggesting that ICP0 is not disrupting the integrity of PML-NBs in this system. To further investigate the effect of ICP0 on the colocalization of latent viral genomes to PML-NBs, we generated an EdC-labeled ICP0-null mutant strain n212 (Cai & Schaffer, 1989) and rescue (Lee *et al*, 2016) verified by immunofluorescence (Fig EV4G) and found that the presence or absence of ICP0 had no detectable impact on the ability of ν DNA foci to colocalize to PML-NBs (Fig 5D). Taken together, these data demonstrate that association of latent viral genomes with PML-NBs in peripheral neurons is dependent on the formation of type I IFN-induced PML-NBs and the presence of type I IFN during initial infection and is independent of ICP0 expression.

PML is required for the IFN α -dependent restriction of HSV-1 latency

To determine whether the stable association of viral genomes with PML-NBs directly contributes to the IFN α -dependent restriction of HSV reactivation, we investigated whether PML depletion was sufficient to restore the ability of the latent viral genomes to reactivate. A previous study has shown that PML-dependent recruitment of HIRA to ISG promoters contributes to the upregulation of gene expression as a result of cytokine release in response to HSV infection (McFarlane *et al*, 2019). Although carried out in non-neuronal cells, this study and others (Ulbricht *et al*, 2012; Chen *et al*, 2015; Kim & Ahn, 2015; Scherer *et al*, 2016) suggest that PML itself may contribute to ISG upregulation, so to determine whether PML was indeed required for ISG stimulation in SCG neurons, we carried out RNA deep sequence analysis in IFN α -treated neurons depleted of PML. Postnatal SCG neurons were transduced with lentiviral vectors expressing non-targeting control or PML-targeting shRNAs (shCtrl and shPML, respectively) and then mock treated or treated with

IFN α (600 IU/ml) for 18 h prior to RNA extraction for next-generation sequencing. High-confidence reads were used for gene expression and gene ontology (GO) analysis. As expected, treatment of shCtrl transduced neurons with IFN α caused large changes in differentially regulated gene expression, with an enrichment of upregulated genes involved in immune system regulation. Similar to control neurons, PML-depleted neurons also significantly upregulated the expression of genes involved in the response to IFN α stimulation. We found that of the total of 248 genes upregulated > 1.5-fold following IFN α treatment, 83.47% of these genes were shared between the shCtrl- and shPML-treated groups (Fig EV5A). Furthermore, we found similar ISG expression (Fig EV5B) and GO pathway enrichment (Fig EV5C). Therefore, in primary SCG neurons, the expression of ISGs in response to exogenous IFN α is largely independent of PML expression.

Because PML depletion did not detectably prevent the induction of type I IFN response genes in SCG neurons, we were able to examine the effect of PML depletion prior to infection on the IFN α -mediated restriction of HSV-1 reactivation. SCG neurons were transduced with lentiviral vectors expressing different PML-targeting shRNA or control non-targeting shRNA. PML depletion was confirmed by average number of PML-NBs per nucleus (Fig 6A) and *Pml* mRNA expression level (Fig EV5D and E) in neurons transduced for 3 days then treated with IFN α (600 IU/ml). As expected, we found a significant decrease in the percent of ν DNA foci stably colocalizing with PML-NBs at 8 dpi in the shPML-treated neurons compared to shCtrl-treated neurons (Fig 6B). Furthermore, we assessed reactivation in neurons infected with HSV-1 in the presence or absence of IFN α (150 IU/ml) at 3 days post-transduction. In these experiments, neurons were infected with a Us11-GFP gH-null virus, which is defective in cell-to-cell spread and eliminates the need for WAY-150138 during reactivation. In untreated neurons, we found no difference in reactivation following treatment with LY294002 (Fig 6C and D). In addition, PML depletion had no effect on the number of GFP-positive neurons in the non-reactivated samples, indicating that in this system that PML was not required for the establishment of latency. However, in neurons treated with IFN α at the time of initial infection, depletion of PML using either of the three PML shRNAs increased the ability of HSV to reactivate as indicated by a 2.97-, 2.69-, and 3.49-fold increase in GFP-positive neurons following treatment with LY294002, respectively (Fig 6E and F). Moreover, there was no significant difference between the PML-depleted, IFN α -treated neurons and the non-IFN α -treated neurons, indicating that PML depletion fully restored the ability of HSV to reactivate from type I IFN-treated neurons. Taken together, these data demonstrate that type I IFN exposure solely at the time of infection results in entrapment of viral genomes in PML-NBs and restricts reactivation. This suggests that genome entrapment by PML promotes a more restrictive or deeper form of latency where reactivation is limited.

Depletion of PML after the establishment of latency enhances reactivation in IFN α -treated neurons

To explore the long-term effect of stable PML-NB-association on the latent viral genome, we next tested whether PML depletion after the establishment of latency was sufficient to restore the ability of the latent viral genomes to reactivate following treatment with a trigger that may directly disrupt PML-NBs. Arsenic trioxide

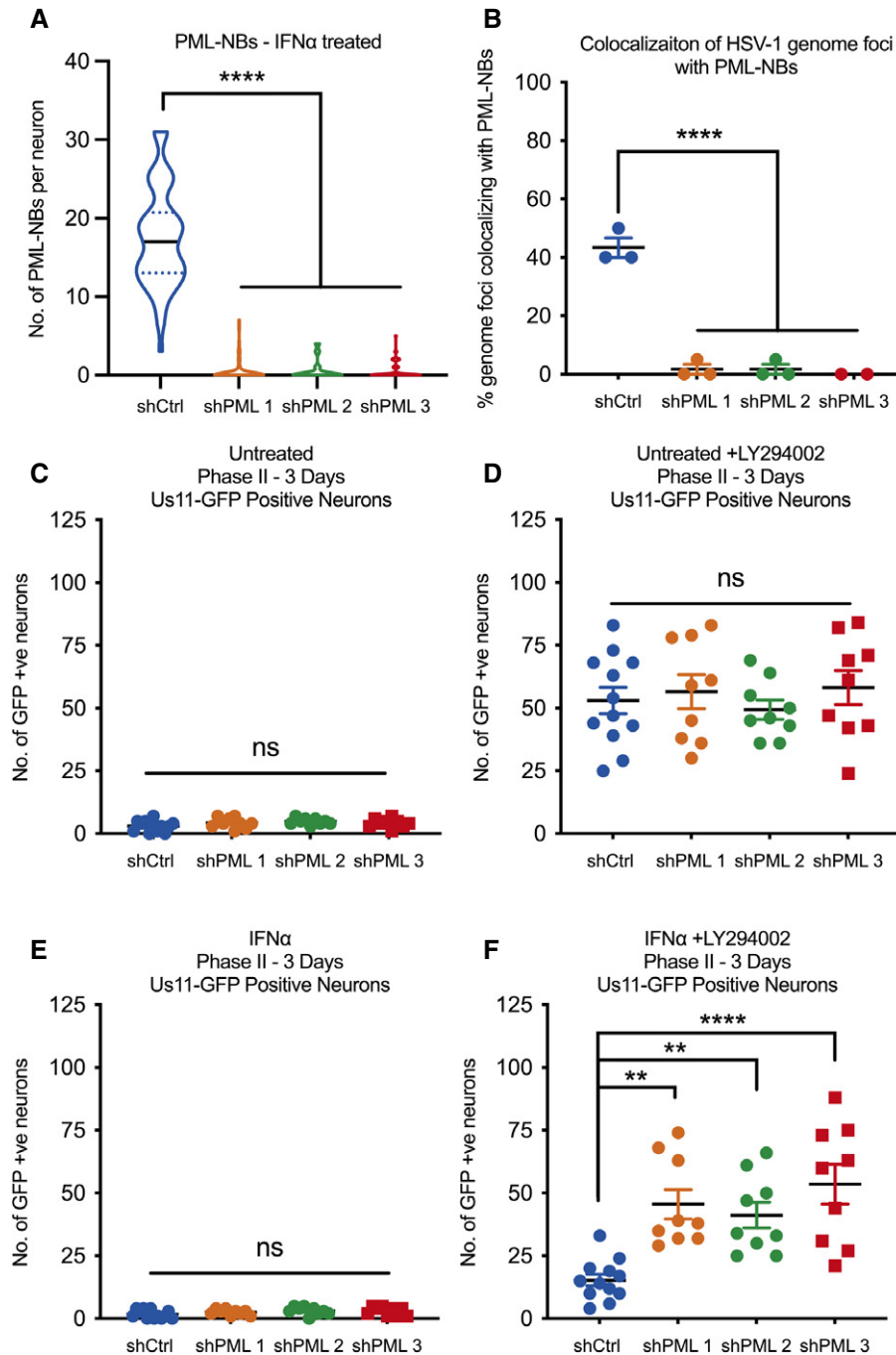


Figure 6. Depletion of PML with shRNA-mediated knockdown prior to infection restores HSV-1 reactivation in type I interferon-treated primary sympathetic neurons.

- A** Quantification of PML puncta in P6 SCG neurons transduced with either control non-targeting shRNA or shRNA targeting PML for 3 days, then treated with IFN α (600 IU/ml) for 18 h. $n = 60$ cells from 3 biological replicates.
- B** Quantification of colocalization of vDNA foci detected by click chemistry to PML in primary SCG neurons transduced with shRNA targeting PML for 3 days prior to being infected with HSV-1^{EdC} in the presence or absence of IFN α (150 IU/ml). Each point represents the percentage of 20 vDNA foci that colocalized to PML from 3 biological replicates.
- C–F** Number of Us11-GFP expressing neurons at 3 days post-LY294002-induced reactivation in P6 SCG neuronal cultures transduced with shRNA targeting PML for 3 days prior to infection with HSV-1 in the presence or absence of IFN α (150 IU/ml). $n = 9$ biological replicates.

Data information: Data represent the mean \pm SEM. Statistical comparisons were made using a one-way ANOVA with Tukey's multiple comparison (ns not significant, ** $p < 0.01$, **** $p < 0.0001$).

Source data are available online for this figure.

(ATO) has been shown to bind directly to PML and disrupt PML-NBs (Lallemend-Breitenbach *et al*, 2008; Zhang *et al*, 2010; Sides *et al*, 2011), and we confirmed that ATO (1 μ M) fully disrupted IFN α -induced PML-NBs in our peripheral neurons by 18 h post-treatment (Fig EV5F). When we investigated reactivation in neurons that were latently infected in the presence or absence of IFN α , then treated with arsenic trioxide (ATO) at 8 dpi, we found that ATO is a very potent stimulator of reactivation independent of IFN α treatment, indicating that ATO is capable of triggering reactivation of genomes that are either PML-NB-associated or not (Fig EV5G). This is likely because ATO is a potent activator of the cell stress response and can result in robust histone phosphorylation (Gehani *et al*, 2010), which we have previously linked to reactivation (Cliffe *et al*, 2015). Although ATO could also induce reactivation in the presence of IFN α -induced PML-NBs, this reactivation was still less robust than mock-treated neurons, likely reflecting the time required for disruption of PML-NBs by ATO.

Therefore, to more specifically determine whether PML depletion restored the ability of neurons to reactivate following treatment with a physiological stimulus of reactivation, neurons were infected with Us11-GFP gH-null HSV-1 virus in the presence or absence of IFN α (150 IU/ml) and subsequently transduced with lentiviral vectors expressing PML-targeting shRNA or control non-targeting shRNA at 1 dpi. Under these experimental conditions, PML knockdown post-infection did not impact LY294002-induced reactivation in untreated neurons (Fig 7A and C), but did increase the ability of HSV to reactivate from IFN α -treated neurons in response to treatment with LY294002, as indicated by a 1.3-fold increase in GFP-positive neurons, albeit reactivation was not restored to levels seen in untreated neurons (Fig 7B and D). As expected, we found that only a small proportion of vDNA foci stably colocalize with PML-NBs at 8 dpi in the shPML-treated neurons compared to vDNA foci in the shCtrl-treated neurons (Fig 7E). Therefore, PML depletion post-infection does not result in detectable spontaneous reactivation of PML-NB-associated viral genomes, indicating that they are still in a repressed state and/or lack the necessary factors required to initiate gene expression. However, depletion of PML does partially restore the ability of HSV to enter the lytic from IFN-treated neurons in response to a reactivation stimulus.

Previously, we have shown that reactivation in response to LY294002 is dependent on activation of the neuronal stress pathway involved dual-leucine zipper kinase (DLK) and JNK activation (Cliffe *et al*, 2015). To test whether the same cell stress stimuli is required to induce reactivation from genomes released from PML-NBs upon shRNA-mediated knockdown of PML, we reactivated in the presence of the DLK inhibitor GNE-3511 (Patel *et al*, 2015). GNE-3511 inhibited LY294002-mediated reactivation of latent genomes following PML depletion post-infection (Fig 7F). Therefore, PML-NBs maintain a restricted form of latency that is more refractory to reactivation, and following PML depletion, viral genomes do not undergo detectable spontaneous reactivation and are still dependent on activation of neuronal cell stress signaling pathways for reactivation.

Discussion

The considerable heterogeneity observed at the neuronal level in the colocalization of viral genomes with different nuclear domains

may reflect in different types of latency that are more or less susceptible to reactivation. The determinants of this heterogeneity and a direct link between the subnuclear localization of a latent genome and its ability to reactivate following a given stimulus was not known. Using a primary neuronal model of HSV latency and reactivation, we found that the presence of type I IFN solely at that time of initial infection acts as a key mediator of the subnuclear distribution of latent viral genomes in neurons and promotes a more restricted form of latency that is less capable of reactivation following disruption of NGF signaling. Importantly, we show that activation of the type I IFN signaling pathway in peripheral neurons induces the detectable formation of PML-NBs, which stably entrap a proportion of latent genomes. Importantly, we show that this IFN-dependent restriction is mediated by PML, suggesting that PML-NBs are directly responsible for the observed restriction of reactivation.

PML-NBs typically number 1–30 bodies per nucleus in non-neuronal cells (Bernardi & Pandolfi, 2007). In the mouse nervous system, however, *Pml* mRNA expression levels have previously been found to be low as measured by *in situ* hybridization (Gray *et al*, 2004). PML protein is enriched in neural progenitor cells, but the induction of differentiation results in the downregulation of PML both at a transcriptional and protein level, and *Pml* mRNA expression is undetectable in post-mitotic neurons in many regions of the developing brain (Regad *et al*, 2009). Our findings in postnatal peripheral neurons further support these observations. *Pml* expression in adult mouse neurons varies considerably between brain regions but is generally confined to the gray matter (Hall *et al*, 2016). Although implicated to play a role in regulating circadian rhythms (Miki *et al*, 2012), synaptic plasticity (Bloomer *et al*, 2007) and the response to toxic proteins that cause neurodegenerative disorders (Yamada *et al*, 2001; Kumada *et al*, 2002; Mackenzie *et al*, 2006; Chort *et al*, 2013), PML regulation, and function in adult nervous system is still largely unknown. In our study, we could not detect PML-NBs in adult primary neurons isolated from the SCG or the TG. In contrast to our findings, PML-NBs have previously been shown to be present in adult mouse and human TG neurons by FISH and immunofluorescence (Catez *et al*, 2012; Maroui *et al*, 2016). However, no quantification was done in these studies, and Catez *et al*, (2012) describe subpopulations of adult TG neurons that did not display any PML signal in the nucleus. In addition, characterization of PML distribution in adult TG neurons by IF-FISH of ganglia isolated *in vivo* may reflect prior exposure to type I IFNs or other signaling molecules. The functional significance of peripheral neurons lacking PML-NBs is unclear, but could be linked to the capacity of neurons to undergo dynamic rearrangement of local and global nuclear architecture during maturation or neuronal excitation. An absence of PML-NBs in neurons could also contribute to their resistance to apoptosis, as PML has also been shown to play a role in cell death through the induction of both p53-dependent and p53-independent apoptotic pathways (Quignon *et al*, 1998; Wang *et al*, 1998; Guo *et al*, 2000). Whether PML-mediated regulation of these pathways occurs in the context of PML-NBs or by PML itself is unclear, but interestingly, the pro-apoptotic functions of Daxx, a PML-NB-associated protein, may require localization to PML-NBs in certain cell types (Croxtton *et al*, 2006). Furthermore, our *in vitro* model using pure populations of intact neurons is devoid of the immune responses and complexities of intact animals, and we cannot rule out the possibility that

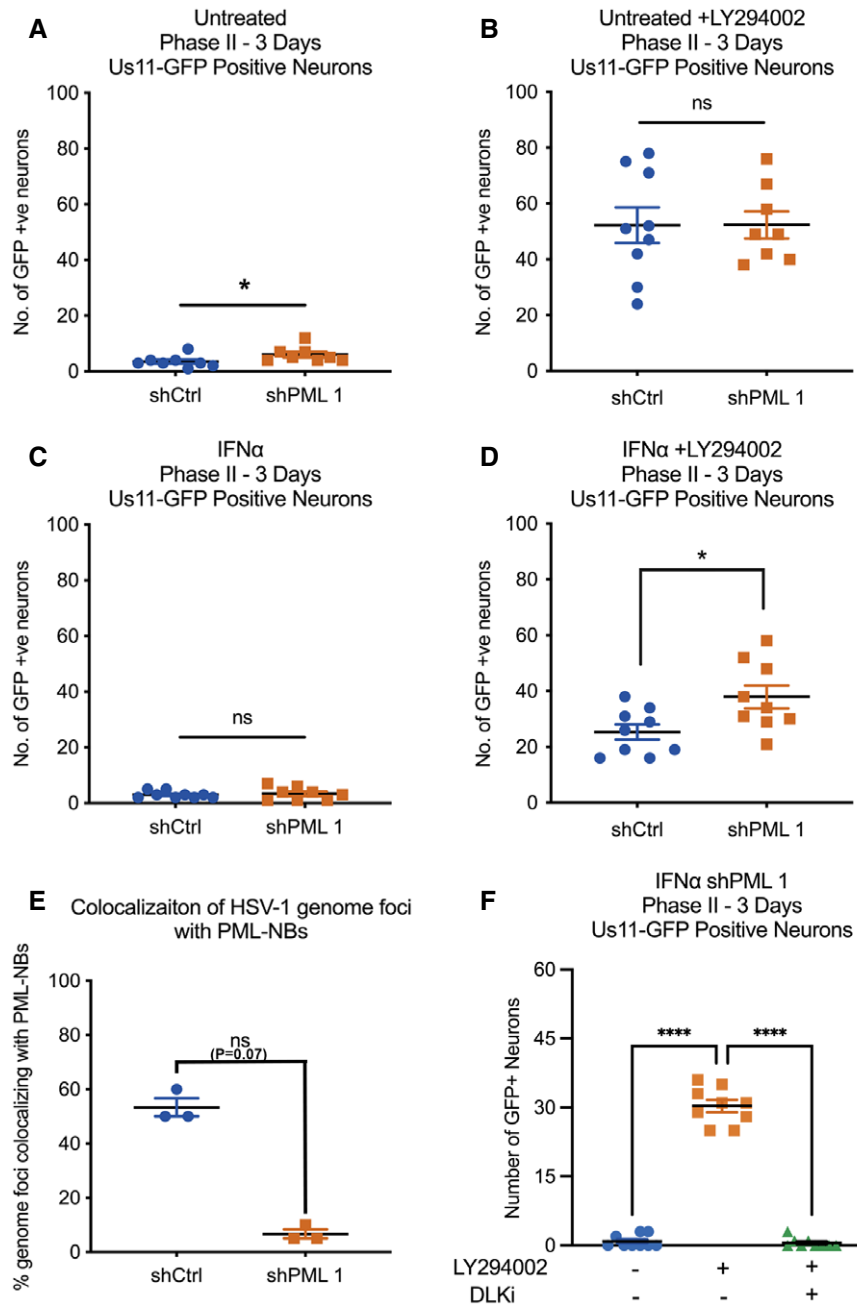


Figure 7. Depletion of PML with shRNA-mediated knockdown post-infection partially restores LY294002-mediated HSV-1 reactivation in type I interferon-treated primary sympathetic neurons.

A–D Number of Us11-GFP expressing neurons at 3 days post-LY294002-induced reactivation in P6 SCG neuronal cultures transduced with shRNA targeting PML at 1 day post-infection with HSV-1 in the presence or absence of IFN α (150 IU/ml). $n = 9$ biological replicates. Statistical comparisons were made using a Mann–Whitney test (ns not significant, $*P < 0.05$).

E Quantification of colocalization of vDNA foci detected by click chemistry to PML in primary SCG neurons transduced with shRNA targeting PML at 1 day post-infection with HSV-1^{E_{dc}} in the presence or absence of IFN α (150 IU/ml). Each point represents the percentage of 20 vDNA foci that colocalized to PML from 3 biological replicates.

F Number of Us11-GFP expressing neurons at 3 days post-reactivation in P6 SCG neuronal cultures transduced with shRNA targeting PML at 1 day post-infection with HSV-1 in the presence of IFN α (150 IU/ml). Reactivation was induced by LY294002 in the presence of the DLK inhibitor GNE-3511 (4 μ M). $n = 9$ biological replicates.

Data information: Data represent the mean \pm SEM. Statistical comparisons were made using a Mann–Whitney test (A–E) or a one-way ANOVA with Tukey’s multiple comparison (F) (ns not significant, $*P < 0.05$, $****P < 0.0001$).

Source data are available online for this figure.

axotomy or the processing of the neurons *ex vivo* could lead to PML-NB disruption or dispersal. However, notwithstanding these caveats, primary neurons provide an excellent model system to understand the impact of extrinsic immune factors and PML-NBs to the altering the nature of HSV latency.

Peripheral neurons are capable of responding to type I IFN signaling, given the robust induction in ISG expression and formation of PML-NBs following treatment with IFN α , and this is supported by a number of previous studies (Yordy *et al*, 2012; Katzenell & Leib, 2016; Song *et al*, 2016; Linderman *et al*, 2017; Barragan-Iglesias *et al*, 2020). Importantly, however, peripheral neurons produce little to no type I interferons upon HSV infection (Yordy *et al*, 2012; Rosato & Leib, 2014), indicating that IFN production arises from other surrounding infected cells. Infected fibroblasts at the body surface, as well as professional immune cells, have been shown to produce high levels of IFN α/β after HSV infection (Hochrein *et al*, 2004; Li *et al*, 2006; Rasmussen *et al*, 2007; Rasmussen *et al*, 2009). In addition, there is evidence of elevated type I IFN in peripheral ganglia during HSV-1 infection (Carr *et al*, 1998), suggesting that glial or immune cells located adjacent to peripheral neuron cell bodies are capable of type I IFN production. It will be important to delineate if the inflammatory environment at the initial site of infection acts on neuronal axons to prime the neuron for a more repressed latent infection or if inflammatory cytokines in the ganglia are crucial for promoting a more repressive state. Although responsive to IFN, primary peripheral and cortical mouse neurons have previously been shown to have inefficient type I IFN-mediated antiviral protection compared to non-neuronal mitotic cells (Yordy *et al*, 2012; Kreit *et al*, 2014). One study showed that DRG neurons are less responsive to type I IFN signaling and used an absence of cell death upon IFN treatment as one of their criteria (Yordy *et al*, 2012). It should be noted that different cell types display specific responses to type I IFN signaling and peripheral neurons have even been reported to be more protected from cell death stimuli following IFN treatment (Chang *et al*, 1990). Furthermore, a previous study found that inducible reactivation of HSV-1 from latently infected neuronal cultures is transiently sensitive to type I IFNs (Linderman *et al*, 2017). Our model of HSV-1 latency and reactivation in primary sympathetic neurons highlights a type I IFN response that is PML-dependent and suggests a role for neuronal IFN signaling in promoting a more restricted latent HSV-1 infection.

Prior to this study, it was not clear whether viral genomes associated with PML-NBs were capable of undergoing reactivation. In response to inhibition of NGF signaling, our data demonstrate that PML-NB-associated genomes are more restricted for reactivation given that (i) IFN induces PML-NB formation and increased association with viral genomes with PML-NBs, (ii) IFN pretreatment promotes restriction of viral reactivation, and (iii) the ability of viral genomes to reactivate from IFN-treated neurons increases with PML knockdown either prior to or following infection. Previous work by Cohen *et al* (2018) showed that quiescent genomes associated with PML-NBs in fibroblasts can be transcriptionally reactivated by induced expression of ICP0. However, this previous study did not address the capability of viral genomes to reactivate in the absence of viral lytic protein (i.e., during reactivation from latency in neurons). In a further study using primary neurons, treatment of quiescently infected neurons with the histone deacetylase inhibitor, trichostatin A (TSA), could lead to disruption of PML-NBs and

induce active viral transcription in a subset of PML-NB-associated genomes (Maroui *et al*, 2016). However, the mechanisms of reactivation following TSA treatment are not known and may be directed via altering the HSV chromatin structure or indirect via increasing the acetylation levels of histones or non-histone proteins, including PML. How increased acetylation relates to the physiological triggers that induce HSV reactivation is not clear. In contrast, loss of neurotrophic signaling can occur in response to known physiological stimuli that trigger HSV reactivation (Suzich & Cliffe, 2018). Although we cannot rule out the possibility that different stimuli have the potential for PML-NB-associated genomes to undergo reactivation, this study clearly demonstrates that at least one well-characterized trigger of reactivation cannot efficiently induce PML-NB-associated genomes to undergo transcription.

Our results identify a persistence of PML-NBs, an IFN-mediated innate immune response, that allows for long-term restriction of latent viral genomes in the absence of continued ISG expression. Interestingly, type I IFN-induced PML-NBs persisted for up to 15 days post-treatment both in the presence and in the absence of viral infection. Given the absence of PML-NBs in our untreated peripheral neurons, this induction and persistence could represent neuron-specific innate immune memory. The persistence of PML-NBs in neurons may alter the subsequent response to IFN and/or viral infection, and it will be interesting to determine whether there is trained immunity in neurons such that subsequent responses differ from the first exposure. What is clear from our results, however, is the role of PML and IFN exposure in sustained repression of the latent HSV genome. Even in the absence of known chromatin changes that occur on the PML-associated viral genome, this long-term effect on the ability of the HSV-1 genome to respond to an exogenous signal and restriction of reactivation is reminiscent of the classical definition of an epigenetic change (of course in the case of post-mitotic neurons in the absence of inheritance).

Here, we demonstrate that there are different types of HSV latency dependent on the subnuclear positioning of the viral genome and ability to reactivate. Genomes associated with PML-NBs are one form of restricted latency in our system. PML-NBs are known to play a role in the restriction of viral gene expression in non-neuronal cells, but the potential mechanism of PML-NB-mediated HSV gene silencing in neurons is unknown. During latency, the viral genome is enriched with histone post-translational modifications (PTMs) consistent with repressive heterochromatin, including H3K9me2/3 and H3K27me3, and it is possible that PML-NBs play a role in the association of viral genomes with core histones, repressive PTMs, or heterochromatin-associated proteins (Wang *et al*, 2005; Cliffe *et al*, 2009; Kwiatkowski *et al*, 2009), or instead via physical compaction of the viral genome in PML-NBs. Although PML-NBs promote a more restricted form of latency, we have shown that latency can be established in the absence of IFN treatment and PML-NBs. Even in IFN-treated neurons, only a proportion of the latent viral genomes colocalized with PML-NBs. This indicates that latent genomes associate with other subnuclear regions and proteins that may promote the assembly and/or maintenance of repressive heterochromatic histone modifications. This supports previous observations that HSV-1 viral genomes also colocalize with centromeric repeats and other, undefined nuclear domains in latently infected TG *in vivo* (Catez *et al*, 2012). For example, the viral genome is known to be enriched for H3K27me3 (Wang *et al*, 2005;

Cliffe *et al*, 2009; Kwiatkowski *et al*, 2009), which can be bound by Polycomb group proteins. Interestingly, we have found that the multifunctional, chromatin remodeler protein ATRX has abundant nuclear staining in neurons and, in contrast to non-neuronal cells, is localized outside of PML-NBs. ATRX staining overlapped with Hoechst DNA staining in our primary neurons, suggesting its localization with AT-rich heterochromatin regions (Bucevicius *et al*, 2019). Ultimately, the latent viral genomes are likely bound by ATRX, Polycomb group proteins, or other repressive cellular proteins independently of PML-NBs. Investigating the identity, mechanism of targeting, and role of these proteins in the induction and maintenance of latency will ultimately facilitate the development of antiviral therapeutics that target the latent stage of infection to prevent reactivation.

Materials and Methods

Reagents

Compounds used in the study are as follows: Acycloguanosine, FUDR, LY 294002, Nerve Growth Factor 2.5S (Alomone Labs), Primocin (Invivogen), Aphidicolin (AG Scientific), IFN- α (EMD Millipore IF009), IFN- β (EMD Millipore IF011), IFN- γ (EMD Millipore IF005), and IFN- λ 2 (PeproTech 250-33); WAY-150138 was kindly provided by Pfizer, Dr. Jay Brown and Dr. Dan Engel at the University of Virginia, and Dr. Lynn Enquist at Princeton University. Compound information and concentrations used can be found below in Table 1.

Preparation of HSV-1 virus stocks

HSV-1 stocks of eGFP-Us11 Patton were grown and titrated on Vero cells obtained from the American Type Culture Collection

(Manassas, VA). Cells were maintained in Dulbecco's modified Eagle's medium (Gibco) supplemented with 10% FetalPlex (Gemini Bio-Products) and 2 mM L-Glutamine. eGFP-Us11 Patton (HSV-1 Patton strain with eGFP reporter protein fused to true late protein Us11 (Benboudjema *et al*, 2003)) was kindly provided by Dr. Ian Mohr at New York University.

StayPut Us11-GFP was created by inserting an eUs11-GFP tag into the previously created gH-deficient HSV-1 SCgHZ virus (strain SC16) through co-transfection of SCgHZ viral DNA and pSXZY-eGFP-Us11 plasmid (Forrester *et al*, 1992). StayPut Us11-GFP is propagated and titrated on previously constructed Vero F6 cells, which contain copies of the gH gene under the control of an HSV-1 gD promoter, as described in Forrester *et al*, (1992). Vero F6s are maintained in Dulbecco's modified Eagle's medium (Gibco) supplemented with 10% FetalPlex (Gemini Bio-Products). They are selected with the supplementation of 250 μ g/mL of G418/Geneticin (Gibco).

Primary neuronal cultures

Sympathetic neurons from the Superior Cervical Ganglia (SCG) of post-natal day 0-2 (P0-P2) or adult (P21-P24) CD1 Mice (Charles River Laboratories) were dissected as previously described (Cliffe *et al*, 2015). Sensory neurons from trigeminal ganglia (TG) of post-natal day 0-2 (P0-P2) CD1 mice (Charles River Laboratories) were dissected using the same protocol. Sensory neurons from TG of adult were dissected as previously described (Bertke *et al*, 2011) with a modified purification protocol using Percoll from the protocol published by Malin *et al* (2007). Rodent handling and husbandry were carried out under animal protocols approved by the Animal Care and Use Committee of the University of Virginia (UVA). Ganglia were briefly kept in Leibovitz's L-15 media with 2.05 mM L-glutamine before dissociation in collagenase type IV (1 mg/ml) followed by trypsin (2.5 mg/ml) for 20 min each at 37°C. Dissociated ganglia were triturated, and approximately 10,000 neurons per well were plated onto rat tail collagen in a 24-well plate. Sympathetic neurons were maintained in CM1 (Neurobasal[®] Medium supplemented with PRIME-XV IS21 Neuronal Supplement (Irvine Scientific), 50 ng/ml Mouse NGF 2.5S, 2 mM L-Glutamine, and Primocin). Aphidicolin (3.3 μ g/ml) was added to the CM1 for the first five days post-dissection to select against proliferating cells. Sensory neurons were maintained in the same media supplemented with GDNF (50 ng/ml; PeproTech 450-44).

Establishment and reactivation of latent HSV-1 infection in primary neurons

Latent HSV-1 infection was established in P6-8 sympathetic neurons from SCGs. Neurons were cultured for at least 24 h without antimetabolic agents prior to infection. The cultures were infected with eGFP-Us11 (Patton recombinant strain of HSV-1 expressing an eGFP reporter fused to true late protein Us11) or StayPut. Neurons were infected at a multiplicity of infection (MOI) of 7.5 PFU/cell with eGFP-Us11 and at an MOI of 5 PFU/cell with StayPut (assuming 1.0×10^4 neurons/well/24-well plate) in DPBS + CaCl₂ + MgCl₂ supplemented with 1% fetal bovine serum, 4.5 g/l glucose, and 10 μ M Acyclovir (ACV) for 2–3 h at 37°C. Post-infection, inoculum was replaced with CM1 containing 50 μ M ACV and an anti-mouse

Table 1. Compounds used and concentrations.

Compound	Supplier	Identifier	Concentration
Acycloguanosine	Millipore Sigma	A4669	10 μ M, 50 μ M
FUDR	Millipore Sigma	F-0503	20 μ M
L-Glutamic Acid	Millipore Sigma	G5638	3.7 μ g/ml
LY 294002	Tocris	1130	20 μ M
IFN α	EMD Millipore	IF009	150 IU/ml, 600 IU/ml
IFN β	EMD Millipore	IF011	150 IU/ml
IFN γ	EMD Millipore	IF005	150 IU/ml, 500 IU/ml
IFN λ 2	PeproTech	250-33	100 ng/ml, 500 ng/ml
NGF 2.5S	Alomone Labs	N-100	50 ng/ml
Primocin	Invivogen	ant-pm-1	100 μ g/ml
Aphidicolin	AG Scientific	A-1026	3.3 μ g/ml
WAY-150138	Pfizer	N/A	10 μ g/ml
AFDye 555 Azide Plus	Click Chemistry Tools	1479-1	10 μ M

IFNAR1 antibody (Leinco Tech I-1188, 1:1,000) for 5–6 days, followed by CM1 without ACV. Reactivation was carried out in DMEM/F12 (Gibco) supplemented with 10% fetal bovine serum, Mouse NGF 2.5S (50 ng/ml), and Primocin. WAY-150138 (10 µg/ml) was added to reactivation cocktail to limit cell-to-cell spread. Reactivation was quantified by counting number of GFP-positive neurons or performing reverse transcription–quantitative PCR (RT–qPCR) of HSV-1 lytic mRNAs isolated from the cells in culture.

Analysis of mRNA expression by reverse transcription–quantitative PCR (RT–qPCR)

To assess relative expression of HSV-1 lytic mRNA, total RNA was extracted from approximately 1.0×10^4 neurons using the Quick-RNA™ Miniprep Kit (Zymo Research) with an on-column DNase I digestion. mRNA was converted to cDNA using the SuperScript IV First-Strand Synthesis system (Invitrogen) using random hexamers for first-strand synthesis and equal amounts of RNA (20–30 ng/reaction). To assess viral DNA load, total DNA was extracted from approximately 1.0×10^4 neurons using the Quick-DNA™ Miniprep Plus Kit (Zymo Research). qPCR was carried out using Power SYBR™ Green PCR Master Mix (Applied Biosystems). The relative mRNA or DNA copy number was determined using the comparative C_T ($\Delta\Delta C_T$) method normalized to mRNA or DNA levels in latently infected samples. Viral RNAs were normalized to mouse reference gene GAPDH. All samples were run in duplicate on an Applied Biosystems™ QuantStudio™ 6 Flex Real-Time PCR System and the mean fold change compared to the reference gene calculated. Primers used are described in Table 2.

Immunofluorescence

Neurons were fixed for 15 min in 4% formaldehyde and blocked in 5% bovine serum albumin and 0.3% Triton X-100 and incubated

overnight in primary antibody. Antibodies used are described in Table 3. Following primary antibody treatment, neurons were incubated for one hour in Alexa Fluor® 488-, 555-, and 647-conjugated secondary antibodies for multi-color imaging (Invitrogen). Nuclei were stained with Hoechst 33258 (Life Technologies). Unless indicated otherwise, z-stack images of entire nuclei were acquired using an sCMOS charge-coupled device camera (pco.edge) mounted on a Nikon Eclipse Ti Inverted Epifluorescent microscope and processed into 2D projection images using the NIS-Elements software (Nikon) Extended Depth of Focus (EDF) plug-in. Images were further analyzed and processed using ImageJ.

Click chemistry

For EdC-labeled HSV-1 virus infections, an MOI of 5 was used. EdC-labeled virus was prepared using a previously described method (McFarlane *et al*, 2019). Click chemistry was carried out as described previously (Alandijany *et al*, 2018) with some modifications. Neurons were washed with CSK buffer (10 mM HEPES, 100 mM NaCl, 300 mM Sucrose, 3 mM MgCl₂, 5 mM EGTA) and simultaneously fixed and permeabilized for 10 min in 1.8% methanol-free formaldehyde (0.5% Triton X-100, 1%

Table 3. Antibodies used for immunofluorescence and concentrations

Antibody	Supplier	Identifier/RRID	Concentration
Anti-PML Mouse monoclonal	EMD Millipore	MAB3738 AB_2166836	1:200
Anti-Beta-III Tubulin Chicken polyclonal	Millipore sigma	AB9354 AB_570918	1:500
Anti-ATRX Rabbit polyclonal	Santa Cruz Bio	sc-15408 AB_2061023	1:250
Anti-Daxx Mouse monoclonal	Santa Cruz Bio	sc-8043 AB_627405	1:250
Anti-STAT1 Rabbit monoclonal	Cell Signaling Technologies	14994 AB_2737027	1:400
Anti-Mx1/2/3 Mouse monoclonal	Santa Cruz Bio	sc-166412 AB_2147714	1:250
Anti-HSV-1 ICP0 Mouse monoclonal	East Coast Bio	H1A027	1:200
Anti-SUMO-1 Rabbit monoclonal	Abcam	Ab32058 AB_778173	1:250
Anti-IFNAR1 Mouse monoclonal	Leinco Tech	I-1188 AB_2830518	1:1,000
F(ab') ₂ Anti-Mouse IgG Alexa Fluor® 555 Goat polyclonal	Thermo Fisher	A21425 AB_2535846	1:1,000
F(ab') ₂ Anti-Rabbit IgG Alexa Fluor® 488 Goat polyclonal	Thermo Fisher	A11070 AB_2534114	1:1,000
F(ab') ₂ Anti-Rabbit IgG Alexa Fluor® 488 Goat polyclonal	Thermo Fisher	A11017 AB_2534084	1:1,000
Anti-Chicken IgY Alexa Fluor® 647 Goat polyclonal	Abcam	ab150175 AB_2732800	1:1,000

Table 2. Primers used for RT–qPCR.

Primer	Sequence 5'–3'
mGAP 1SF	CAT GGC CTT CCG TGT GTT CCT A
mGAP 1SR	GCG GCA CGT CAG ATC CA
ICP27 F	GCA TCC TTC GTG TTT GTC ATT CTG
ICP27 R	GCA TCT TCT CTC CGA CCC CG
ICP8 1SF	GGA GGT GCA CCG CAT ACC
ICP8 1SR	GGC TAA AAT CCG GCA TGA AC
gC #1 F	GAG TTT GTC TGG TTC GAG GAC
gC #1R	ACG GTA GAG ACT GTG GTG AA
PML F	GGG AAA CAG AGG AGC GAG TT
PML R	AAG GCC TTG AGG GAA TTG GG
ISG15 F	CAA GCA GCC AGA AGC AGA CT
ISG15 R	CCC AGC ATC TTC ACC TTT AGG
IRF7 F	CCA GTT GAT CCG CAT AAG GT
IRF7 R	GAG GCT CAC TTC TTC CCT ATT T
LAT F	TGT GTG GTG CCC GTG TCT T
LAT R	CCA GCC AAT CCG TGT CGG

phenylmethylsulfonyl fluoride (PMSF)) in CSK buffer, then washed twice with PBS before continuing to the click chemistry reaction and immunostaining. Samples were blocked with 3% BSA for 30 min, followed by click chemistry using EdC-labeled HSV-1 DNA and the Click-iT EdU Alexa Flour 555 Imaging Kit (Thermo Fisher Scientific, C10638) according to the manufacturer's instructions with AFDye 555 Picolyl Azide (Click Chemistry Tools, 1288). For immunostaining, samples were incubated overnight with primary antibodies in 3% BSA. Following primary antibody treatment, neurons were incubated for one hour in Alexa Fluor® 488- and 647-conjugated secondary antibodies for multi-color imaging (Invitrogen). Nuclei were stained with Hoechst 33258 (Life Technologies). Epifluorescence microscopy images were acquired at 60× using an sCMOS charge-coupled device camera (pco.edge) mounted on a Nikon Eclipse Ti Inverted Epifluorescent microscope using NIS-Elements software (Nikon). Images were analyzed and processed using ImageJ. Confocal microscopy images were acquired using a Zeiss LSM 880 confocal microscope using the 63× Plan-Apochromat oil immersion lens (numerical aperture 1.4) using 405, 488, 543, and 633 nm laser lines. Zen black software (Zeiss) was used for image capture, generating cut mask channels, and calculating weighted colocalization coefficients. Exported images were processed with minimal adjustment using Adobe Photoshop and assembled for presentation using Adobe Illustrator.

Preparation of lentiviral vectors

Lentiviruses expressing shRNA against PML (PML-1 TRCN0000229547, PML-2 TRCN0000229549, PML-3 TRCN0000314605), or a control lentivirus shRNA (Everett *et al*, 2006) were prepared by co-transfection with psPAX2 and pCMV-VSV-G (Stewart *et al*, 2003) using the 293LTV packaging cell line (Cell Biolabs). Supernatant was harvested at 40- and 64-h post-transfection. Sympathetic neurons were transduced overnight in neuronal media containing 8µg/ml protamine and 50 µM ACV.

RNA sequence analysis

Reads were checked for quality using FASTQC (v0.11.8), trimmed using BBMAP (v3.8.16b), and aligned to the mouse genome with GENCODE (vM22) annotations using STAR (v2.7.1a). Transcripts per million calculations were performed by RSEM (v1.3.1), the results of which were imported into R (v4.0.2) and Bioconductor (v3.12) using tximport (v1.18.0). Significant genes were called using DESeq2, using fold change cutoffs and p-value cutoffs of 0.5 and 0.05, respectively. Results were visualized using Heatplus (v2.36.0), PCATools (v2.2.0), and UpSetR (v1.4.0). Functional enrichment was performed using GSEA and Metascape.

Statistical analysis

Power analysis was used to determine the appropriate sample sizes for statistical analysis. All statistical analysis was performed using Prism V8.4. A Mann–Whitney test was used for all experiments where the group size was 2. All other experiments were analyzed using a one-way ANOVA with Tukey's multiple comparison. Specific analyses are included in the figure legends. For all reactivation experiments measuring GFP expression, viral DNA, gene

expression, or DNA load, individual biological replicates were plotted (an individual well of primary neurons) and all experiments were repeated from pools of neurons from at least 3 litters.

Data availability

The RNA-seq dataset generated and analyzed in the current study is available at the NCBI Gene Expression omnibus (accession number GSE166738; <https://www.ncbi.nlm.nih.gov/geo/query/acc.cgi?acc=GSE166738>).

Expanded View for this article is available online.

Acknowledgements

We thank Dr. Ian Mohr at New York University for the gift of the Us11-GFP virus and Gary Cohen at the University of Pennsylvania for SCgHZ. This work was supported by R21AI151340 (ARC), R01NS105630 (ARC), The Owens Family Foundation (ARC), NIH/NEI F30EY030397 (JBS), NIH/NIAID T32AI007046 (JBS and SRC), T32GM007267 (JBS), NIH/NIGMS T32GM008136 (SD) and MRC (<https://mrc.ukri.org>) MC_UU_12014/5 (CB).

Author contributions

JBS: Conceptualization, formal analysis, investigation, methodology, validation, visualization, writing—original draft, writing—review and editing. SRC: Investigation, validation. HB: Investigation. SD: Investigation, validation. EK: Data curation, formal analysis, methodology, software. ARS: Investigation. AB: Investigation. CB: Resources, writing—review and editing. ARC: Conceptualization, formal analysis, funding acquisition, investigation, validation, methodology, project administration, supervision, validation, visualization, writing—original draft, writing—review and editing.

Conflict of interest

The authors declare that they have no conflict of interest.

References

- Alandijany T, Roberts APE, Conn KL, Loney C, McFarlane S, Orr A, Boutell C (2018) Distinct temporal roles for the promyelocytic leukaemia (PML) protein in the sequential regulation of intracellular host immunity to HSV-1 infection. *PLoS Pathog* 14: e1006769
- Baringer JR, Pisani P (1994) Herpes simplex virus genomes in human nervous system tissue analyzed by polymerase chain reaction. *Ann Neurol* 36: 823–829
- Baringer JR, Swoveland P (1973) Recovery of herpes-simplex virus from human trigeminal ganglions. *N Engl J Med* 288: 648–650
- Barragan-Iglesias P, Franco-Enzastiga U, Jeevakumar V, Shiers S, Wangzhou A, Granados-Soto V, Campbell ZT, Dussor G, Price TJ (2020) Type I interferons act directly on nociceptors to produce pain sensitization: implications for viral infection-induced pain. *J Neurosci* 40: 3517–3532
- Benboudjema L, Mulvey M, Gao Y, Pimplikar SW, Mohr I (2003) Association of the herpes simplex virus type 1 Us11 gene product with the cellular kinesin light-chain-related protein PAT1 results in the redistribution of both polypeptides. *J Virol* 77: 9192–9203
- Bernardi R, Pandolfi PP (2007) Structure, dynamics and functions of promyelocytic leukaemia nuclear bodies. *Nat Rev Mol Cell Biol* 8: 1006–1016

- Bertke AS, Swanson SM, Chen J, Imai Y, Kinchington PR, Margolis TP (2011) A5-positive primary sensory neurons are nonpermissive for productive infection with herpes simplex virus 1 in vitro. *J Virol* 85: 6669–6677
- Bishop CL, Ramalho M, Nadkarni N, May Kong W, Higgins CF, Krauzewicz N (2006) Role for centromeric heterochromatin and PML nuclear bodies in the cellular response to foreign DNA. *Mol Cell Biol* 26: 2583–2594
- Bloomer WA, VanDongen HM, VanDongen AM (2007) Activity-regulated cytoskeleton-associated protein Arc/Arg3.1 binds to spectrin and associates with nuclear promyelocytic leukemia (PML) bodies. *Brain Res* 1153: 20–33
- Boutell C, Cuchet-Lourenco D, Vanni E, Orr A, Glass M, McFarlane S, Everett RD (2011) A viral ubiquitin ligase has substrate preferential SUMO targeted ubiquitin ligase activity that counteracts intrinsic antiviral defence. *PLoS Pathog* 7: e1002245
- Boutell C, Sadis S, Everett RD (2002) Herpes simplex virus type 1 immediate-early protein ICPO and is isolated RING finger domain act as ubiquitin E3 ligases in vitro. *J Virol* 76: 841–850
- Bucevicius J, Keller-Findeisen J, Gilat T, Hell SW, Lukinavicius G (2019) Rhodamine-Hoechst positional isomers for highly efficient staining of heterochromatin. *Chem Sci* 10: 1962–1970
- Cabral JM, Oh HS, Knipe DM (2018) ATRX promotes maintenance of herpes simplex virus heterochromatin during chromatin stress. *Elife* 7: e40228
- Cai WZ, Schaffer PA (1989) Herpes simplex virus type 1 ICPO plays a critical role in the de novo synthesis of infectious virus following transfection of viral DNA. *J Virol* 63: 4579–4589
- Camarena V, Kobayashi M, Kim JY, Roehm P, Perez R, Gardner J, Wilson AC, Mohr I, Chao MV (2010) Nature and duration of growth factor signaling through receptor tyrosine kinases regulates HSV-1 latency in neurons. *Cell Host Microbe* 8: 320–330
- Carr DJ, Veress LA, Noisakran S, Campbell IL (1998) Astrocyte-targeted expression of IFN- α 1 protects mice from acute ocular herpes simplex virus type 1 infection. *J Immunol* 161: 4859–4865
- Catez F, Picard C, Held K, Gross S, Rousseau A, Theil D, Sawtell N, Labetoulle M, Lomonte P (2012) HSV-1 genome subnuclear positioning and associations with host-cell PML-NBs and centromeres regulate LAT locus transcription during latency in neurons. *PLoS Pathog* 8: e1002852
- Chang JY, Martin DP, Johnson Jr EM (1990) Interferon suppresses sympathetic neuronal cell death caused by nerve growth factor deprivation. *J Neurochem* 55: 436–445
- Chelbi-Alix MK, Pelicano L, Quignon F, Koken MH, Venturini L, Stadler M, Pavlovic J, Degos L, de The H (1995) Induction of the PML protein by interferons in normal and APL cells. *Leukemia* 9: 2027–2033
- Chelbi-Alix MK, de The H (1999) Herpes virus induced proteasome-dependent degradation of the nuclear bodies-associated PML and Sp100 proteins. *Oncogene* 18: 935–941
- Chen SH, Kramer MF, Schaffer PA, Coen DM (1997) A viral function represses accumulation of transcripts from productive-cycle genes in mouse ganglia latently infected with herpes simplex virus. *J Virol* 71: 5878–5884
- Chen Y, Wright J, Meng X, Leppard KN (2015) Promyelocytic Leukemia Protein Isoform II Promotes Transcription Factor Recruitment To Activate Interferon Beta and Interferon-Responsive Gene Expression. *Mol Cell Biol* 35: 1660–1672
- Chort A, Alves S, Marinello M, Dufresnois B, Dornbierer J-G, Tesson C, Latouche M, Baker DP, Barkats M, El Hachimi KH et al (2013) Interferon beta induces clearance of mutant ataxin 7 and improves locomotion in SCA7 knock-in mice. *Brain* 136: 1732–1745
- Cliffe AR, Arbuckle JH, Vogel JL, Geden MJ, Rothbart SB, Cusack CL, Strahl BD, Kristie TM, Deshmukh M (2015) Neuronal stress pathway mediating a histone Methyl/Phospho switch is required for herpes simplex virus reactivation. *Cell Host Microbe* 18: 649–658
- Cliffe AR, Coen DM, Knipe DM (2013) Kinetics of facultative heterochromatin and polycomb group protein association with the herpes simplex viral genome during establishment of latent infection. *MBio* 4: e00590-12
- Cliffe AR, Garber DA, Knipe DM (2009) Transcription of the herpes simplex virus latency-associated transcript promotes the formation of facultative heterochromatin on lytic promoters. *J Virol* 83: 8182–8190
- Cliffe AR, Knipe DM (2008) Herpes simplex virus ICPO promotes both histone removal and acetylation on viral DNA during lytic infection. *J Virol* 82: 12030–12038
- Cliffe AR, Wilson AC (2017) Restarting lytic gene transcription at the onset of herpes simplex virus reactivation. *J Virol* 91: e01419-16
- Clynes D, Higgs DR, Gibbons RJ (2013) The chromatin remodeller ATRX: a repeat offender in human disease. *Trends Biochem Sci* 38: 461–466
- Cohen C, Corpet A, Roubille S, Maroui MA, Pocard N, Rousseau A, Kleijwegt C, Binda O, Texier P, Sawtell N et al (2018) Promyelocytic leukemia (PML) nuclear bodies (NBs) induce latent/quiescent HSV-1 genomes chromatinization through a PML NB/Histone H3.3/H3.3 Chaperone Axis. *PLoS Pathog* 14: e1007313
- Croxtan R, Puto LA, de Belle I, Thomas M, Torii S, Hanaii F, Cuddy M, Reed JC (2006) Daxx represses expression of a subset of antiapoptotic genes regulated by nuclear factor- κ B. *Cancer Res* 66: 9026–9035
- Cuchet-Lourenco D, Vanni E, Glass M, Orr A, Everett RD (2012) Herpes simplex virus 1 ubiquitin ligase ICPO interacts with PML isoform I and induces its SUMO-independent degradation. *J Virol* 86: 11209–11222
- Cuddy SR, Schinlever AR, Dochnal S, Seegren PV, Suzich J, Kundu P, Downs TK, Farah M, Desai BN, Boutell C et al (2020) Neuronal hyperexcitability is a DLK-dependent trigger of herpes simplex virus reactivation that can be induced by IL-1. *eLife* 9: e58037
- Du T, Zhou G, Roizman B (2011) HSV-1 gene expression from reactivated ganglia is disordered and concurrent with suppression of latency-associated transcript and miRNAs. *Proc Natl Acad Sci* 108: 18820–18824
- Efstathiou S, Preston CM (2005) Towards an understanding of the molecular basis of herpes simplex virus latency. *Virus Res* 111: 108–119
- Everett RD, Chelbi-Alix MK (2007) PML and PML nuclear bodies: implications in antiviral defence. *Biochimie* 89: 819–830
- Everett RD, Freemont P, Saitoh H, Dasso M, Orr A, Kathoria M, Parkinson J (1998) The disruption of ND10 during herpes simplex virus infection correlates with the Vmw110- and proteasome-dependent loss of several PML isoforms. *J Virol* 72: 6581–6591
- Everett RD, Maul GG (1994) HSV-1 IE protein Vmw110 causes redistribution of PML. *EMBO J* 13: 5062–5069
- Everett RD, Murray J (2005) ND10 components relocate to sites associated with herpes simplex virus type 1 nucleoprotein complexes during virus infection. *J Virol* 79: 5078–5089
- Everett RD, Murray J, Orr A, Preston CM (2007) Herpes simplex virus type 1 genomes are associated with ND10 nuclear substructures in quiescently infected human fibroblasts. *J Virol* 81: 10991–11004
- Everett RD, Parada C, Gripon P, Sirma H, Orr A (2008) Replication of ICPO-null mutant herpes simplex virus type 1 is restricted by both PML and Sp100. *J Virol* 82: 2661–2672
- Everett RD, Rechter S, Papior P, Tavalai N, Stamminger T, Orr A (2006) PML contributes to a cellular mechanism of repression of herpes simplex virus type 1 infection that is inactivated by ICPO. *J Virol* 80: 7995–8005
- Everett RD, Sourvinos G, Leiper C, Clements JB, Orr A (2004) Formation of nuclear foci of the herpes simplex virus type 1 regulatory protein ICP4 at early times of infection: localization, dynamics, recruitment of ICP27, and

- evidence for the de novo induction of ND10-like complexes. *J Virol* 78: 1903–1917
- Forrester A, Farrell H, Wilkinson G, Kaye J, Davis-Poynter N, Minson T (1992) Construction and properties of a mutant of herpes simplex virus type 1 with glycoprotein H coding sequences deleted. *J Virol* 66: 341–348
- Garber DA, Schaffer PA, Knipe DM (1997) A LAT-associated function reduces productive-cycle gene expression during acute infection of murine sensory neurons with herpes simplex virus type 1. *J Virol* 71: 5885–5893
- Garrick D, Samara V, McDowell TL, Smith AJ, Dobbie L, Higgs DR, Gibbons RJ (2004) A conserved truncated isoform of the ATR-X syndrome protein lacking the SWI/SNF-homology domain. *Gene* 326: 23–34
- Gehani SS, Agrawal-Singh S, Dietrich N, Christophersen NS, Helin K, Hansen K (2010) Polycomb group protein displacement and gene activation through MSK-dependent H3K27me3S28 phosphorylation. *Mol Cell* 39: 886–900
- Gordon YJ, Romanowski EG, Araullo-Cruz T, Kinchington PR (1995) The proportion of trigeminal ganglionic neurons expressing herpes simplex virus type 1 latency-associated transcripts correlates to reactivation in the New Zealand rabbit ocular model. *Graefes Arch Clin Exp Ophthalmol* 233: 649–654
- Gray PA, Fu H, Luo P, Zhao Q, Yu J, Ferrari A, Tenzen T, Yuk DI, Tsung EF, Cai Z et al (2004) Mouse brain organization revealed through direct genome-scale TF expression analysis. *Science* 306: 2255–2257
- Greger JG, Katz RA, Ishov AM, Maul GG, Skalka AM (2005) The cellular protein daxx interacts with avian sarcoma virus integrase and viral DNA to repress viral transcription. *J Virol* 79: 4610–4618
- Grotzinger T, Jensen K, Will H (1996) The interferon (IFN)-stimulated gene Sp100 promoter contains an IFN-gamma activation site and an imperfect IFN-stimulated response element which mediate type I IFN inducibility. *J Biol Chem* 271: 25253–25260
- Guo A, Salomoni P, Luo J, Shih A, Zhong S, Gu W, Pandolfi PP (2000) The function of PML in p53-dependent apoptosis. *Nat Cell Biol* 2: 730–736
- Hall MH, Magalska A, Malinowska M, Ruszczycycki B, Czaban I, Patel S, Ambrožek-Latecka M, Zołocińska E, Broszkiewicz H, Parobczak K et al (2016) Localization and regulation of PML bodies in the adult mouse brain. *Brain Struct Funct* 221: 2511–2525
- Hendricks RL, Weber PC, Taylor JL, Koumbis A, Tumpey TM, Glorioso JC (1991) Endogenously produced interferon alpha protects mice from herpes simplex virus type 1 corneal disease. *J Gen Virol* 72(Pt. 7): 1601–1610
- Hill JM, Sedarati F, Javier RT, Wagner EK, Stevens JG (1990) Herpes simplex virus latent phase transcription facilitates in vivo reactivation. *Virology* 174: 117–125
- Hochrein H, Schlatter B, O’Keeffe M, Wagner C, Schmitz F, Schiemann M, Bauer S, Suter M, Wagner H (2004) Herpes simplex virus type-1 induces IFN-alpha production via Toll-like receptor 9-dependent and -independent pathways. *Proc Natl Acad Sci USA* 101: 11416–11421
- Ives AM, Bertke AS (2017) Stress hormones epinephrine and corticosterone selectively modulate herpes simplex virus 1 (HSV-1) and HSV-2 productive infections in adult sympathetic, but not sensory, neurons. *J Virol* 91: e00582-17
- Jones CA, Fernandez M, Herc K, Bosnjak L, Miranda-Saksena M, Boadle RA, Cunningham A (2003) Herpes simplex virus type 2 induces rapid cell death and functional impairment of murine dendritic cells in vitro. *J Virol* 77: 11139–11149
- Kamada R, Yang W, Zhang Y, Patel MC, Yang Y, Ouda R, Dey A, Wakabayashi Y, Sakaguchi K, Fujita T et al (2018) Interferon stimulation creates chromatin marks and establishes transcriptional memory. *Proc Natl Acad Sci* 115: E9162–E9171
- Katzenell S, Leib DA (2016) Herpes simplex virus and interferon signaling induce novel autophagic clusters in sensory neurons. *J Virol* 90: 4706–4719
- Kim JY, Mandarin A, Chao MV, Mohr I, Wilson AC (2012) Transient reversal of episome silencing precedes VP16-dependent transcription during reactivation of latent HSV-1 in neurons. *PLoS Pathog* 8: e1002540
- Kim YE, Ahn JH (2015) Positive role of promyelocytic leukemia protein in type I interferon response and its regulation by human cytomegalovirus. *PLoS Pathog* 11: e1004785
- Knipe DM, Cliffe A (2008) Chromatin control of herpes simplex virus lytic and latent infection. *Nat Rev Microbiol* 6: 211–221
- Kobayashi M, Wilson AC, Chao MV, Mohr I (2012) Control of viral latency in neurons by axonal mTOR signaling and the 4E-BP translation repressor. *Genes Dev* 26: 1527–1532
- Kramer MF, Coen DM (1995) Quantification of transcripts from the ICP4 and thymidine kinase genes in mouse ganglia latently infected with herpes simplex virus. *J Virol* 69: 1389–1399
- Kreit M, Paul S, Knoops L, De Cock A, Sorgeloos F, Michiels T (2014) Inefficient type I interferon-mediated antiviral protection of primary mouse neurons is associated with the lack of apolipoprotein I9 expression. *J Virol* 88: 3874–3884
- Kumada S, Uchihara T, Hayashi M, Nakamura A, Kikuchi E, Mizutani T, Oda M (2002) Promyelocytic leukemia protein is redistributed during the formation of intranuclear inclusions independent of polyglutamine expansion: an immunohistochemical study on Marinesco bodies. *J Neuropathol Exp Neurol* 61: 984–991
- Kwiatkowski DL, Thompson HW, Bloom DC (2009) The polycomb group protein Bmi1 binds to the herpes simplex virus 1 latent genome and maintains repressive histone marks during latency. *J Virol* 83: 8173–8181
- Lallemant-Breitenbach V, Jeanne M, Benhenda S, Nasr R, Lei M, Peres L, Zhou J, Zhu J, Raught B, de The H (2008) Arsenic degrades PML or PML-RARalpha through a SUMO-triggered RNF4/ubiquitin-mediated pathway. *Nat Cell Biol* 10: 547–555
- Lallemant-Breitenbach V, de The H (2010) PML nuclear bodies. *Cold Spring Harb Perspect Biol* 2: a000661
- Lee JS, Raja P, Knipe DM (2016) Herpesviral ICPO protein promotes two waves of heterochromatin removal on an early viral promoter during lytic infection. *MBio* 7(1): e02007-15.
- Leib DA, Bogard CL, Kosz-Vnenchak M, Hicks KA, Coen DM, Knipe DM, Schaffer PA (1989) A deletion mutant of the latency-associated transcript of herpes simplex virus type 1 reactivates from the latent state with reduced frequency. *J Virol* 63: 2893–2900
- Lewis PW, Elsaesser SJ, Noh K-M, Stadler SC, Allis CD (2010) Daxx is an H3.3-specific histone chaperone and cooperates with ATRX in replication-independent chromatin assembly at telomeres. *Proc Natl Acad Sci USA* 107: 14075–14080
- Li H, Zhang J, Kumar A, Zheng M, Atherton SS, Yu FS (2006) Herpes simplex virus 1 infection induces the expression of proinflammatory cytokines, interferons and TLR7 in human corneal epithelial cells. *Immunology* 117: 167–176
- Linderman JA, Kobayashi M, Rayannavar V, Fak JJ, Darnell RB, Chao MV, Wilson AC, Mohr I (2017) Immune escape via a transient gene expression program enables productive replication of a latent pathogen. *Cell Rep* 18: 1312–1323
- Lukashchuk V, Everett RD (2010) Regulation of ICPO-null mutant herpes simplex virus type 1 infection by ND10 components ATRX and hDaxx. *J Virol* 84: 4026–4040

- Ma JZ, Russell TA, Spelman T, Carbone FR, Tschärke DC (2014) Lytic gene expression is frequent in HSV-1 latent infection and correlates with the engagement of a cell-intrinsic transcriptional response. *PLoS Pathog* 10: e1004237
- Mackenzie IR, Baker M, West G, Woulfe J, Qadi N, Gass J, Cannon A, Adamson J, Feldman H, Lindholm C et al (2006) A family with tau-negative frontotemporal dementia and neuronal intranuclear inclusions linked to chromosome 17. *Brain* 129: 853–867
- Malin SA, Davis BM, Molliver DC (2007) Production of dissociated sensory neuron cultures and considerations for their use in studying neuronal function and plasticity. *Nat Protoc* 2: 152–160
- Maroui MA, Callé A, Cohen C, Streichenberger N, Texier P, Takissian J, Rousseau A, Pocard N, Welsch J, Corpet A et al (2016) Latency entry of herpes simplex virus 1 is determined by the interaction of its genome with the nuclear environment. *PLoS Pathog* 12: e1005834–e1005828
- Maul GG (1998) Nuclear domain 10, the site of DNA virus transcription and replication. *BioEssays* 20: 660–667
- Maul GG, Ishov AM, Everett RD (1996) Nuclear domain 10 as preexisting potential replication start sites of herpes simplex virus type-1. *Virology* 217: 67–75
- McFarlane S, Orr A, Roberts APE, Conn KL, Iliev V, Loney C, da Silva Filipe A, Smollett K, Gu Q, Robertson N et al (2019) The histone chaperone HIRA promotes the induction of host innate immune defences in response to HSV-1 infection. *PLoS Pathog* 15: e1007667
- Miki T, Xu Z, Chen-Goodspeed M, Liu M, Van Oort-Jansen A, Rea MA, Zhao Z, Lee CC, Chang KS (2012) PML regulates PER2 nuclear localization and circadian function. *EMBO J* 31: 1427–1439
- Mikloska Z, Cunningham AL (2001) Alpha and gamma interferons inhibit herpes simplex virus type 1 infection and spread in epidermal cells after axonal transmission. *J Virol* 75: 11821–11826
- Mikloska Z, Danis VA, Adams S, Lloyd AR, Adrian DL, Cunningham AL (1998) In vivo production of cytokines and beta (C-C) chemokines in human recurrent herpes simplex lesions—do herpes simplex virus-infected keratinocytes contribute to their production? *J Infect Dis* 177: 827–838
- Moorlag S, Roring RJ, Joosten LAB, Netea MG (2018) The role of the interleukin-1 family in trained immunity. *Immunol Rev* 281: 28–39
- Muller S, Matunis MJ, Dejean A (1998) Conjugation with the ubiquitin-related modifier SUMO-1 regulates the partitioning of PML within the nucleus. *EMBO J* 17: 61–70
- Nicoll MP, Hann W, Shivkumar M, Harman LE, Connor V, Coleman HM, Proenca JT, Efstathiou S (2016) The HSV-1 latency-associated transcript functions to repress latent phase lytic gene expression and suppress virus reactivation from latently infected neurons. *PLoS Pathog* 12: e1005539
- Noh KM, Maze I, Zhao D, Xiang B, Wenderski W, Lewis PW, Shen L, Li H, Allis CD (2015) ATRX tolerates activity-dependent histone H3 methyl/phosphorylation switching to maintain repetitive element silencing in neurons. *Proc Natl Acad Sci USA* 112: 6820–6827
- Patel S, Cohen F, Dean BJ, De La Torre K, Deshmukh G, Estrada AA, Ghosh AS, Gibbons P, Gustafson A, Huestis MP et al (2015) Discovery of dual leucine zipper kinase (DLK, MAP3K12) inhibitors with activity in neurodegeneration models. *J Med Chem* 58: 401–418
- Peng GC, Jones C, Ciacci-Zanella J, Stone M, Henderson G, Yukht A, Slanina SM, Hofman FM, Ghiasi H, Nesburn AB et al (2000) Virus-induced neuronal apoptosis blocked by the herpes simplex virus latency-associated transcript. *Science* 287: 1500–1503
- Proenca JT, Coleman HM, Connor V, Winton DJ, Efstathiou S (2008) A historical analysis of herpes simplex virus promoter activation in vivo reveals distinct populations of latently infected neurones. *J Gen Virol* 89: 2965–2974
- Quignon F, De Bels F, Koken M, Feunteun J, Ameisen JC, de The H (1998) PML induces a novel caspase-independent death process. *Nat Genet* 20: 259–265
- Rasmussen SB, Jensen SB, Nielsen C, Quartin E, Kato H, Chen ZJ, Silverman RH, Akira S, Paludan SR (2009) Herpes simplex virus infection is sensed by both Toll-like receptors and retinoic acid-inducible gene-like receptors, which synergize to induce type I interferon production. *J Gen Virol* 90: 74–78
- Rasmussen SB, Sorensen LN, Malmgaard L, Ank N, Baines JD, Chen ZJ, Paludan SR (2007) Type I interferon production during herpes simplex virus infection is controlled by cell-type-specific viral recognition through Toll-like receptor 9, the mitochondrial antiviral signaling protein pathway, and novel recognition systems. *J Virol* 81: 13315–13324
- Regad T, Bellodi C, Nicotera P, Salomoni P (2009) The tumor suppressor Pml regulates cell fate in the developing neocortex. *Nat Neurosci* 12: 132–140
- Richter ER, Dias JK, Gilbert II JE, Atherton SS (2009) Distribution of herpes simplex virus type 1 and varicella zoster virus in ganglia of the human head and neck. *J Infect Dis* 200: 1901–1906
- Rosato PC, Leib DA (2014) Intrinsic innate immunity fails to control herpes simplex virus and vesicular stomatitis virus replication in sensory neurons and fibroblasts. *J Virol* 88: 9991–10001
- Sainz Jr B, Halford WP (2002) Alpha/Beta interferon and gamma interferon synergize to inhibit the replication of herpes simplex virus type 1. *J Virol* 76: 11541–11550
- Sawtell NM (1997) Comprehensive quantification of herpes simplex virus latency at the single-cell level. *J Virol* 71: 5423–5431
- Scherer M, Otto V, Stump JD, Klingl S, Muller R, Reuter N, Muller H, Stamminger T (2016) Characterization of recombinant human cytomegaloviruses encoding IE1 mutants L174P and 1–382 reveals that viral targeting of PML bodies perturbs both intrinsic and innate immune responses. *J Virol* 90: 1190–1205
- Shalginskikh N, Poleshko A, Skalka AM, Katz RA (2013) Retroviral DNA methylation and epigenetic repression are mediated by the antiviral host protein Daxx. *J Virol* 87: 2137–2150
- Sides MD, Block GJ, Shan B, Esteves KC, Lin Z, Flemington EK, Lasky JA (2011) Arsenic mediated disruption of promyelocytic leukemia protein nuclear bodies induces ganciclovir susceptibility in Epstein-Barr positive epithelial cells. *Virology* 416: 86–97
- Song R, Koyuncu OO, Greco TM, Diner BA, Cristea IM, Enquist LW (2016) Two modes of the axonal interferon response limit alphaherpesvirus neuroinvasion. *MBio* 7: e02145–e2215
- Stadler M, Chelbi-Alix MK, Koken MH, Venturini L, Lee C, Saib A, Quignon F, Pelicano L, Guillemin MC, Schindler C et al (1995) Transcriptional induction of the PML growth suppressor gene by interferons is mediated through an ISRE and a GAS element. *Oncogene* 11: 2565–2573
- Stevens JG, Wagner EK, Devi-Rao GB, Cook ML, Feldman LT (1987) RNA complementary to a herpesvirus alpha gene mRNA is prominent in latently infected neurons. *Science* 235: 1056–1059
- Stewart SA, Dykxhoorn DM, Palliser D, Mizuno H, Yu EY, An DS, Sabatini DM, Chen IS, Hahn WC, Sharp PA et al (2003) Lentivirus-delivered stable gene silencing by RNAi in primary cells. *RNA* 9: 493–501
- Suzich JB, Cliffe AR (2018) Strength in diversity: Understanding the pathways to herpes simplex virus reactivation. *Virology* 522: 81–91
- Thompson RL, Sawtell NM (1997) The herpes simplex virus type 1 latency-associated transcript gene regulates the establishment of latency. *J Virol* 71: 5432–5440

- Thompson RL, Sawtell NM (2001) Herpes simplex virus type 1 latency-associated transcript gene promotes neuronal survival. *J Virol* 75: 6660–6675
- Trousdale MD, Steiner I, Spivack JG, Deshmane SL, Brown SM, MacLean AR, Subak-Sharpe JH, Fraser NW (1991) In vivo and in vitro reactivation impairment of a herpes simplex virus type 1 latency-associated transcript variant in a rabbit eye model. *J Virol* 65: 6989–6993
- Ulbricht T, Alzrigat M, Horch A, Reuter N, von Mikecz A, Steimle V, Schmitt E, Kramer OH, Stamminger T, Hemmerich P (2012) PML promotes MHC class II gene expression by stabilizing the class II transactivator. *J Cell Biol* 199: 49–63
- Wang J, Shiels C, Sasieni P, Wu PJ, Islam SA, Freemont PS, Sheer D (2004) Promyelocytic leukemia nuclear bodies associate with transcriptionally active genomic regions. *J Cell Biol* 164: 515–526
- Wang Q-Y, Zhou C, Johnson KE, Colgrove RC, Coen DM, Knipe DM (2005) Herpesviral latency-associated transcript gene promotes assembly of heterochromatin on viral lytic-gene promoters in latent infection. *Proc Natl Acad Sci* 102: 16055–16059
- Wang ZG, Ruggero D, Ronchetti S, Zhong S, Gaboli M, Rivi R, Pandolfi PP (1998) PML is essential for multiple apoptotic pathways. *Nat Genet* 20: 266–272
- Warren KG, Brown SM, Wroblewska Z, Gilden D, Koprowski H, Subak-Sharpe J (1978) Isolation of latent herpes simplex virus from the superior cervical and vagus ganglions of human beings. *N Engl J Med* 298: 1068–1069
- Wilcox CL, Johnson EM (1987) Nerve growth factor deprivation results in the reactivation of latent herpes simplex virus in vitro. *J Virol* 61: 2311–2315
- Wilcox CL, Smith RL, Freed CR, Johnson EM (1990) Nerve growth factor-dependence of herpes simplex virus latency in peripheral sympathetic and sensory neurons in vitro. *J Neurosci* 10: 1268–1275
- Xu P, Roizman B (2017) The SP100 component of ND10 enhances accumulation of PML and suppresses replication and the assembly of HSV replication compartments. *Proc Natl Acad Sci USA* 114: E3823–E3829
- Yamada M, Sato T, Shimohata T, Hayashi S, Igarashi S, Tsuji S, Takahashi H (2001) Interaction between neuronal intranuclear inclusions and promyelocytic leukemia protein nuclear and coiled bodies in CAG repeat diseases. *Am J Pathol* 159: 1785–1795
- Yordy B, Iijima N, Huttner A, Leib D, Iwasaki A (2012) A neuron-specific role for autophagy in antiviral defense against herpes simplex virus. *Cell Host Microbe* 12: 334–345
- van Zeijl M, Fairhurst J, Jones TR, Vernon SK, Morin J, LaRocque J, Feld B, O'Hara B, Bloom JD, Johann SV (2000) Novel class of thiourea compounds that inhibit herpes simplex virus type 1 DNA cleavage and encapsidation: resistance maps to the UL6 gene. *J Virol* 74: 9054–9061
- Zhang XW, Yan XJ, Zhou ZR, Yang FF, Wu ZY, Sun HB, Liang WX, Song AX, Lallemand-Breitenbach V, Jeanne M *et al* (2010) Arsenic trioxide controls the fate of the PML-RARalpha oncoprotein by directly binding PML. *Science* 328: 240–243
- Zhong S, Muller S, Ronchetti S, Freemont PS, Dejean A, Pandolfi PP (2000a) Role of SUMO-1-modified PML in nuclear body formation. *Blood* 95: 2748–2752
- Zhong S, Salomoni P, Pandolfi PP (2000b) The transcriptional role of PML and the nuclear body. *Nat Cell Biol* 2: E85–E90